12-2011

Short Distance Ground Wave Propagation Modeling in Irregular and Forested Environments

Zachary Michael Crane
zcrane@utk.edu

To the Graduate Council:

I am submitting herewith a thesis written by Zachary Michael Crane entitled "Short Distance Ground Wave Propagation Modeling in Irregular and Forested Environments." I have examined the final electronic copy of this thesis for form and content and recommend that it be accepted in partial fulfillment of the requirements for the degree of Master of Science, with a major in Electrical Engineering.

Paul B. Crilly, Major Professor

We have read this thesis and recommend its acceptance:

Aly E. Fathy, Seddik M. Djouadi

Accepted for the Council:
Carolyn R. Hodges

Vice Provost and Dean of the Graduate School

(Original signatures are on file with official student records.)

Short Distance Ground Wave Propagation Modeling in Irregular and Forested Environments

A Thesis Presented for the
Master of Science
Degree
The University of Tennessee, Knoxville

Zachary Michael Crane
December 2011

ACKNOWLEDGEMENTS

I would like to thank Dr. Paul B. Crilly for his generous support of my endeavors. His time, wisdom, and dedication to teaching were invaluable in both the completion of this work and in the pursuit of my undergraduate degree. I am privileged to call him an instructor, mentor, and friend.

I would also like to thank Dr. Stephen F. Smith for providing the opportunity to work at Oak Ridge National Laboratory. Without his willingness to work with students and provide opportunities, this endeavor would not have been possible.

I would like to thank the additional members of my thesis committee, Dr. Seddik M. Djouadi and Dr. Aly Fathy, for taking the time to read, understand, and approve my work. Not only were they kind enough to serve on my committee, but they have both proven to be valuable mentors and instructors throughout my undergraduate and graduate studies.

I would like to thank my mother and father, for always trusting in my abilities and believing in me. Without their wisdom and insight, I would never have completed my B.S., much less my M.S.

Finally, I give thanks for and to my beautiful wife, Shannon, for her care and love during both my coursework and the writing of this work. She is a pillar of strength and wisdom.

ABSTRACT

A model for the phase of a ground wave propagating over irregular and forested terrain has been developed and tested for a transmission system operating at 3.315 MHz.

In this model, the time delay induced beyond that of the standard velocity of radio waves in air is modeled as a combination of 3 effects: the finite conductivity of the earth, the irregularity of the terrain over which the wave is propagating, and the forestation of the terrain.

The finite conductivity model is based on a small curvature formula developed by Van Der Pol and Bremmer. The terrain irregularity model models additional delay as a perturbation of the surface impedance and is a function of the slope angle.

The additional delay due to forestation is modeled as a dissipative dielectric slab which introduces a velocity factor. The foliage on the range was quantized into three levels of density: open, thin, and thick. The foliage thickness was determined manually from commercial satellite imagery.

The ground based network used to measure propagation times consists of 5 perimeter transmitter sites and 5 receiver sites. Results for 1 of the 5 receiver sites have already been obtained. The results accurately predict the additional delay time introduced. The additional delays predicted over the 5 paths vary widely, ranging from 400 to almost 1000 nanoseconds. The lengths of these paths vary between 2 and 3 miles. The relative permittivity of each grade of forest density along each path was found to be in agreement.

The significance of this work revolves around navigating in GPS denied environments, areas of chronic GPS unavailability, such as urban areas, canyons, under dense foliage, or when a GPS signal is being unintentionally or intentionally jammed. In order to provide a path forward to a robust augmentation to GPS, the propagation phenomena associated with ground-based navigation must be understood, and more effectively modeled.

TABLE OF CONTENTS

LIST OF TABLES

Table Page

LIST OF FIGURES

Figure Page

1: INTRODUCTION

Land-based radio navigation systems were the focus of attention for those desiring to navigate by radio long before the advent of GPS. Based on terrestrial transmitters, systems like LORAN and Decca provided relatively accurate and repeatable readings which military and civilians alike relied upon.

However, when GPS became fully operational in the mid-1990's, and particularly after selective availability was deactivated, the unparalleled accuracy and availability of the GPS signal quickly drove other navigation systems to either obscurity or a very distant option of last resort. In the United States, where LORAN was king before GPS, the US Government, seeking to cut costs, deactivated the LORAN system in early 2010, choosing to allocate its yearly operating budget elsewhere.

The unfortunate side effect of this rapid adaptation of GPS has only recently begun to take the attention of those in research, development, and risk management. With no other system being capable of providing the precision of location and time transfer that GPS offers, billions of people risk falling victim to a widespread GPS outage on a daily basis. In fact, the United States Government has designated GPS as a critical infrastructure for transit, time transfer, and defense [1].

This had led to a resurgence of interest in the land-based navigation community and the protection and augmentation which land-based systems can offer to GPS services. To this end, Oak Ridge National Laboratory, in conjunction with graduate researchers at the University of Tennessee, Knoxville, has been conducting research related to ground-based navigation systems, and has established a prototype range and system which utilizes several features which differentiate it from GPS and provide a robust and viable backup to GPS, without sharing failure modes of GPS.

During the initial testing phase of the ORNL system, large discrepancies in predicted versus actual propagation times from transmitter to receiver led to extensive research into ground-wave propagation phenomena. The bulk of this

thesis will be devoted to the explanation of ground-wave propagation theory, the research conducted at ORNL, the model developed, and the results of applying the model.

Before delving into the specifics of the land-based system designed at ORNL, it is useful to return to the analysis of GPS vulnerabilities in order to understand how and why a land-based system can effectively augment and back up the GPS constellation.

1.1: Survey of GPS Vulnerabilities

The root of GPS vulnerability to intentional and unintentional interference lies in its low level of received power. The GPS Standard Positioning Service Specification, produced by the US Government in 1992 during the completion of the GPS system, specifies a received power of -160 dBw at the Earth's surface [2]. While such a small received power is necessary for satellite longevity and interference considerations, this opens up GPS receivers on the ground to a host of interfering phenomena.

Of primary concern in terms of natural interference is a phenomenon known as Ionospheric scintillation. While the effects of scintillation can be mitigated and even eliminated by dual band receivers [3], these receivers are prohibitively expensive for the average citizen to purchase solely for the purpose of navigation [4]. The effects of Ionospheric scintillation can be seen in figure 1. These results, obtained during testing in Bangkok, Thailand, demonstrate that scintillation can produce absolute position error in excess of 20 m.

The advantage of a properly-designed, land-based system should be clear; assuming the system is designed to rely on ground-wave, and not Ionospheric propagation phenomena, any GPS receiver with such a land-based augmentation would be immune to scintillation effects, since the propagating wave does not pass through the ionosphere.

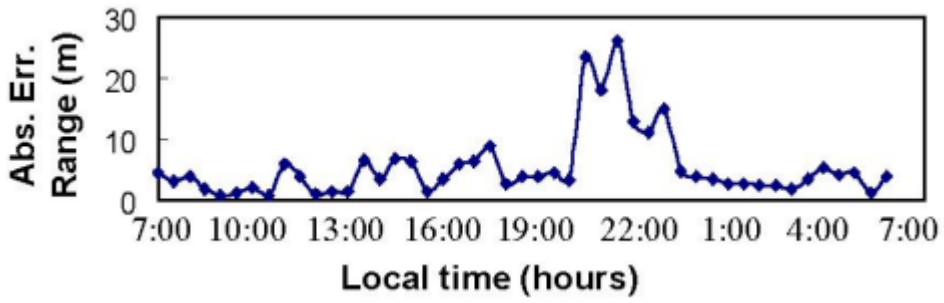

Figure 1 - The absolute range error from GPS signal in scintillation condition (14 April 2003) [5]

Of additional concern is unintentional disruption to GPS through a number of different broadcast channels in adjacent bands. At least one incident involving GPS interference from a Television signal has been observed [6]. Additional studies suggest [7] that Ultra Wideband transmissions which are not properly regulated for signal duration can raise the noise floor sufficiently to cause interference with GPS operations.

While any system is vulnerable to disruption due to RF in adjacent spectral space, GPS is particularly vulnerable due to the incredibly small amount of received power available. Any land-based backup or augmentation capable of higher output power and/or frequency diversity would provide an extra measure of safety against unintentional interference.

While unintentional interference and atmospheric effects are significant concerns, of far greater concern is the possibility of intentional jamming and/or spoofing. The difference between these two intentional disruptive tactics is important to note. Jamming is the intentional broadcast of an interfering signal, generally at a very high power, to interfere with reception of the correct GPS signal. The receiver's front end is either overloaded, or the weak GPS signal is lost in what appears to be overwhelming amounts of noise.

Spoofing is the broadcast of a similar or identical signal to an authentic GPS carrier, except with erroneous location or timing data in the spoofing signal. This leads to the receiver displaying a location or time, but an erroneous one due

to the data contained within the spoofed signal. These two interference tactics will be addressed in order.

Jamming of GPS is certainly possible. While it is illegal to buy, sell, or use GPS jammers in the United States, they are available from various internet retailers, and Ward [8] and Gilmore [9] have demonstrated that it is possible to deny GPS service to a wide area with a low power jammer, provided that it is airborne. It is also important to note that this is for a fairly unsophisticated jammer. A jammer broadcasting a spoofed and spread GPS replica could easily deny service to all users not over the horizon. A “GPS like” signal would pose a much greater threat since it could virtually eliminate the processing gain of a GPS receiver.

It is also important to note that since receiver design is not stringently standardized, receiver responses to jamming can take on a variety of different erroneous behaviors. A receiver may immediately lose lock and report nothing until the jamming has ceased, or error may slowly increase as Signal to Noise ratio decreases. In some cases, large errors just before loss of lock have been reported [10].

The tactic of spoofing, while more complicated than jamming, is hardly impossible to achieve. Since the GPS signal is non-proprietary, there is nothing to stop a malicious entity from producing a GPS waveform containing inaccurate navigation or timing information and transmitting it. Unfortunately, due to the significant danger in even attempting to spoof a GPS signal, there is not a significant amount of data available on actual tests of spoofing equipment.

The threats to GPS due to jamming, spoofing, and atmospheric noise are credible and documented. However, they need not be cause for alarm. In fact, these known threats led the way forward for the design of a viable back-up solution. Knowing the dangers posed to GPS has allowed radio engineers the world over to better understand how to best construct a back-up system in order to mitigate these risks. At Oak Ridge National Laboratory, a land-based

augmentation to GPS has been under development since the early 2000's. This system is known as the Theater Positioning System.

1.2: The Theater Positioning System

The Theater Positioning System (TPS) was designed specifically to augment GPS against some of its most credible threats. Through this overview of the TPS concept, its key features will be highlighted, and it will be shown how TPS was designed to close several of the vulnerabilities associated with GPS. Additionally, this will set the stage to explain the body of research done surrounding propagation phenomena associated with the TPS range.

The first characteristic of note for the TPS system is that it is software defined. Figure 2 shows a basic software defined radio: an RF front end, coupled with A/D and D/A converters and a Field Programmable Gate Array (FPGA) and supporting circuitry.

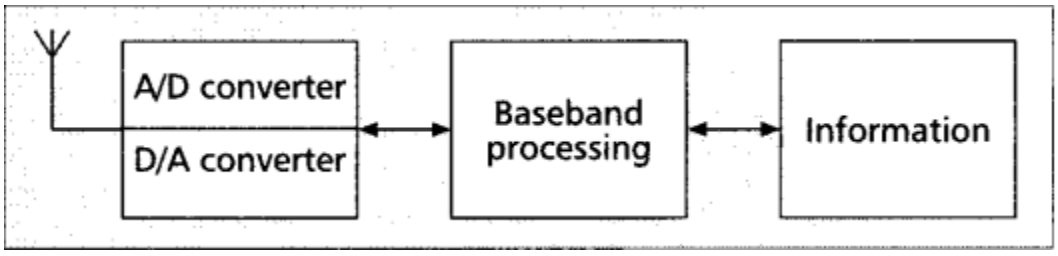

Figure 2 - Basic architecture of a software-defined radio system [11]

Utilizing nothing but software alterations, a software defined radio can change its waveform, operating frequency, and basically any parameter within the operator's imagination without changing hardware. In reference to the threat of spoofing or jamming, an SDR has the capability to completely alter itself to avoid being spoofed or jammed. Whether by changing operating frequency or waveform, an SDR is uniquely suited to avoid interference. Granted, there are transmitter and receiver software updates to manage, but an SDR ceases to be purpose built, and should a malicious party wish to interfere with transmissions

from an SDR, a simple software update can completely alter the manner in which the system operates.

The TPS system is also entirely land-based and relies on ground wave propagation phenomena, as opposed to Ionospheric propagation. Cosmic activity and solar storms will have a much smaller effect on its ability to effectively transmit location data. Ground wave propagation has its own set of challenges, including a much less homogeneous medium to propagate through and over. However, these inhomogeneous regions are much more predictable than solar activity, and extensive research has been done relating the amplitude and phase of a propagating ground wave on both sides of a conductivity alteration. Another advantage of the TPS system being ground-based is that transmitter power can be greatly increased.

The TPS system also operates at relatively low frequency, allowing penetration into buildings, through dense foliage, and into many other areas where GPS signals cannot reach. Thus, an integrated receiver architecture employing both GPS and TPS would have much more consistent coverage in urban environments, under heavy foliage, and in areas subject to large amounts of multipath interference.

Finally, the details of the TPS signal format are, at least currently, proprietary. Without knowledge of a signal's parameters, it is very difficult to effectively spoof this signal. As stated before, the software defined radio format of the TPS system would allow for rapid reconfiguration in the event of a spoofing attack.

An operational TPS setup for a battlefield is shown conceptually in figure 3. The transmitters are deployed away from areas where they could experience physical danger from combat operations in a roughly circular geometry. In a civilian navigation and timing distribution environment, the transmitters would most likely be permanently deployed.

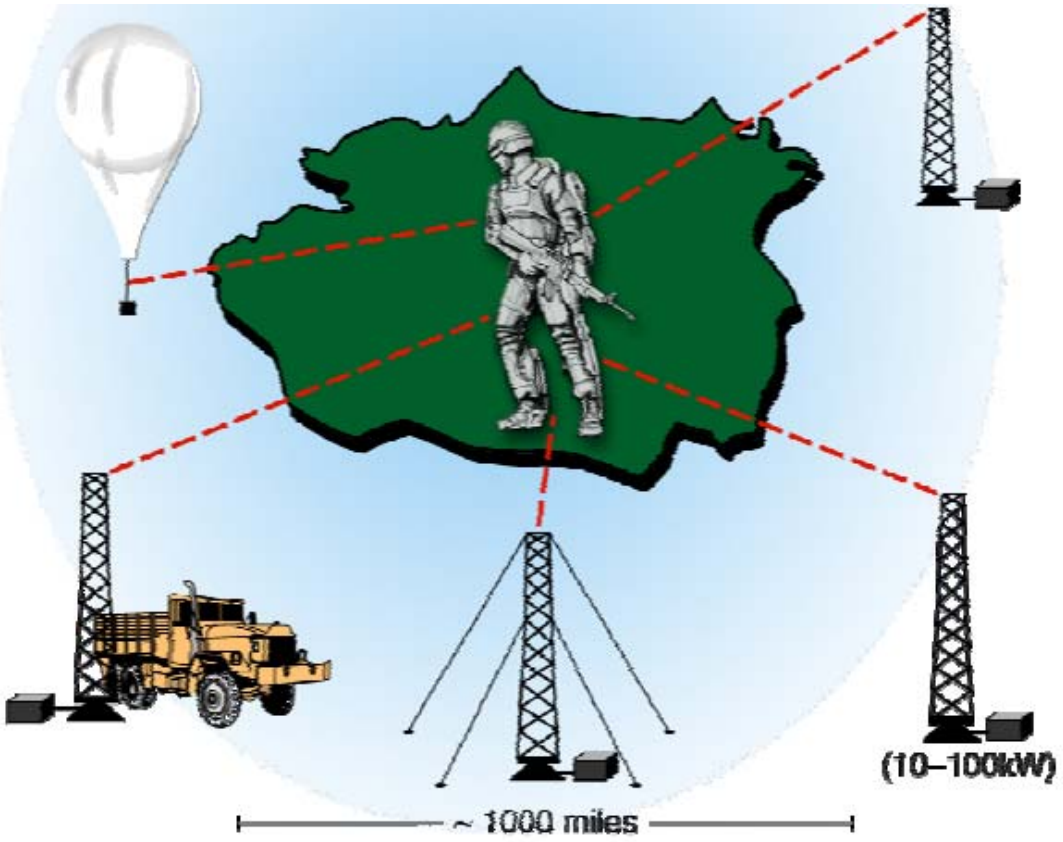

Figure 3 - Typical TPS Deployment in Large Operational Area [12]

1.3: Testing Range and Propagation Discrepancies

The current testing range at Oak Ridge National Laboratory has been designed on a smaller scale than what is planned for an operational TPS deployment. It consists of 5 transmitter sites, with one active, permanent receiver site and 4 additional sites planned once mobile receiver prototypes are ready for operation. The 5 propagation paths in question range in length from 2.15 miles to 3.27 miles, not accounting for great circle corrections or terrain irregularity. These great circle variations and irregularities were considered, however the stated measurements are sufficient for simple introduction to the propagation range. Satellite imagery of the propagation range is shown in figure 4.

Figure 4 - Satellite Imagery of TPS Propagation Range

As will be seen in the body of research, elevation plays a role in perturbing the surface impedance of the earth, and thus will need to be taken into account when considering the propagation characteristics of the terrain. Therefore, elevation data was obtained from a 9 m resolution Digital Terrain Elevation Database (DTED). Profiles of all paths are available in Appendix A.

During initial setup of propagation predictions, a datum velocity of 1.0171 ns/ft was assumed. This is equal to the velocity of light in air. The slowdowns due to terrain roughness, finite conductivity, and possible foliage factors were anticipated [12]. Upon completing the first round of pseudoranges, the discrepancies between the assumed velocity of the propagating wave and the actual velocity were found. These results, along with some statistical analysis of the paths, are shown in table 1. The discrepancy assumed to be due entirely to propagation is shown in red in the rightmost column.

Table 1 - Observed Propagation Times on the ORNL Range

Xmit Position ID	Recv Position ID	Smoothed* Path Distance (ft)	Smoothed Path Delay (ns)	Est. Transmitter Delay (ns)	Total Est. Delay (ns)	Measured Pseudo-range (ns)	Difference [Est. - Meas.] (ns)
1	6	17277.85898711	17573.31	1031	18604.31	19631.237	-1026.926624
2	6	16783.46930407	17070.47	1281	18351.47	18889.237	-537.7703708
3	6	16234.75470323	16512.37	1281	17793.37	18448.237	-654.8679913
4	6	12516.47628095	12730.51	1031	13761.51	14854.237	-1092.728975
5	6	11504.68354178	11701.41	1031	12732.41	13401.237	-668.8233697

The negative sign indicates that the predicted propagation time was less than the measured propagation time. The approximate physical location of these pseudoranges is shown in figure 5. The pseudoranges enclose an area 0.92 miles in perimeter.

The discrepancies between actual propagation velocities and assumed propagation velocities were assumed to consist of 3 effects: the finite conductivity of the earth, the irregularity of the earth, and the foliage coverage. These effects were assumed to be additive. In order to develop a model for each of these effects, relevant literature on each subject will be examined. Some theories have been extracted directly from literature, and some have been built upon to arrive at a solution which agrees with the phenomena observed at ORNL.

Figure 5 – Approximate physical locations of initial pseudoranges relative to TPS receiver site 6

2: LITERATURE REVIEW

Radio transmission over the surface of the earth became a subject of great interest around the turn of the century starting with Marconi's wireless transmissions. Almost as soon as an experimental apparatus was available to begin testing the propagation of electromagnetic waves, physicists and mathematicians began attempting to predict the nature of wireless transmission range and coverage.

2.1: Planar Earth Theory

The first attempt of note was made by Zenneck [13]. He assumed a planar, conducting half space with finite conductivity and some permittivity other than that of free space. The propagating medium above was assumed to be free space and the entire region, both earth and air, assumed nonmagnetic (i.e. with permeability equal to μ_0). The air/ground interface was assumed to be in the x-y plane. For $z > 0$ and $z < 0$ there is a single magnetic field component. Zenneck also established the equation for wave tilt, the effective slowing of the face of the propagating wave due to the finite conductivity of the earth and the $z = 0$ interface. Zenneck's work set the stage for researchers to begin understanding how the air/earth interface guided the propagating wave

Next to attempt to tackle the problem and dealing with actual physical excitations in the form of vertically polarized dipoles, was Arnold Sommerfeld [14]. Sommerfeld covered the subject with extreme mathematical rigor, Sommerfeld also showed that, while the Zenneck solution physically existed, its particular mode was very weakly excited from a localized source such as a single antenna. Sommerfeld also introduced a nomenclature which has become the prevailing practice of most formulations, even up to the present. The adjusted field, which is a function of distance and ground conductivity, is found by multiplying the reference field produced at some distance r over a perfectly

conducting earth with an attenuation function, commonly known as F(p). This nomenclature has survived over almost a century's worth of work, demonstrating the authority and widespread adaptation of Sommerfeld's work.

However, even great scientists such as Sommerfeld were not immune to error. In his original 1909 formulation of his surface wave solutions, it is believed by many that he made a sign error which led to an erroneous belief that the Zenneck surface wave was a major contributor to ground wave propagation. This was corrected in 1926 in a later publication, but provoked significant discussion for many years in the interim and after [15].

The author of much of this discussion was Dr. K.A. Norton. Dr. Norton published numerous works in the proceedings of the IRE. Norton was first a radio engineer, and much of his work revolved around obtaining useful formulae and charts from Sommerfeld's complicated mathematical expressions. Norton studied the subject exhaustively, working with vertical, horizontal, and loop polarizations, and published definitive work on dealing with receiver and transmitter antennas at varying heights [15].

2.2: Spherical Earth Considerations

Before the work of G. N. Watson [16], the spherical nature of the earth was not effectively considered. Watson employed a harmonic series expansion with spherical Bessel functions of integer order, and found that the resulting number of terms necessary to represent the field at close distances was enormous. J.R. Wait describes the procedure Watson used to resolve the problem. "Watson's first step was to represent the series by a contour integral that enclosed the real axis of the complex wave-number plane...which provided a highly convergent residue series. [17]"

Unfortunately, at short distances, even the residue series takes hundreds of terms to converge. Thankfully, a solution to this problem was found by utilizing a modified flat earth solution, This solution, found by Bremmer, is commonly known as a modified flat earth series [18]. It is of particular importance to the

construction of theories for the ORNL range due to the extremely short distances of propagation being considered. The modified flat earth solution converges very quickly for short distances, and is not computationally intensive compared to the residue series derivations. This solution is adequately rigorous for short range propagation predictions such as those found on the ORNL range.

2.3: Inhomogeneous Paths Considered

A final important theoretical consideration is mixed path theory. It plays extensively into magnitude and phase advances over boundaries of conductivity. George Millington was the first to effectively compute the propagation phenomena which occurs at a conductivity boundary [19]. Using excellent intuition, he postulated that a wave propagating over a boundary of conductivities would undergo a “recovery effect” in which magnitude would increase and phase would advance, assuming that the wave was propagating from a region of lower to higher conductivity. While his original results did not behave as he expected, he quickly resolved this problem by taking the geometric mean of the paths in both directions. His results have been experimentally verified in numerous publications and his work is the subject of numerous RF coverage prediction tools [20]. His work was so definitive that the propagation phenomenon, depicted in figure 6 was named Millington Effect.

2.4: Applications Emerge

Up to this point in the literature review, most, if not all considerations have been geared towards predicting field strength and coverage only. This is largely due to the lack of inspiration to utilize the research being done in the early part of the century for radio navigation. However, beginning with World War II and a system code named GEE [21], both the allies and Nazi Germany began using radio to navigate.

Their first attempts were crude, and researchers quickly began to realize that propagation phenomena above and beyond simple distance equals rate

times time were governing the delays associated with their navigation systems. Before long, the work of Wait, Sommerfeld, Millington, and others would become relevant. GEE was a short-lived product of the war. However, it provided the impetus for the most widely implemented, land based navigation system ever designed: LORAN. The LORAN system, designed during WW II and upgraded and maintained throughout the latter half of the 20th century, provided hyperbolic navigation data far and wide, and proved the test bed for the beginnings of propagation predictions the world over. A brief description of the functional operation of LORAN is educational here.

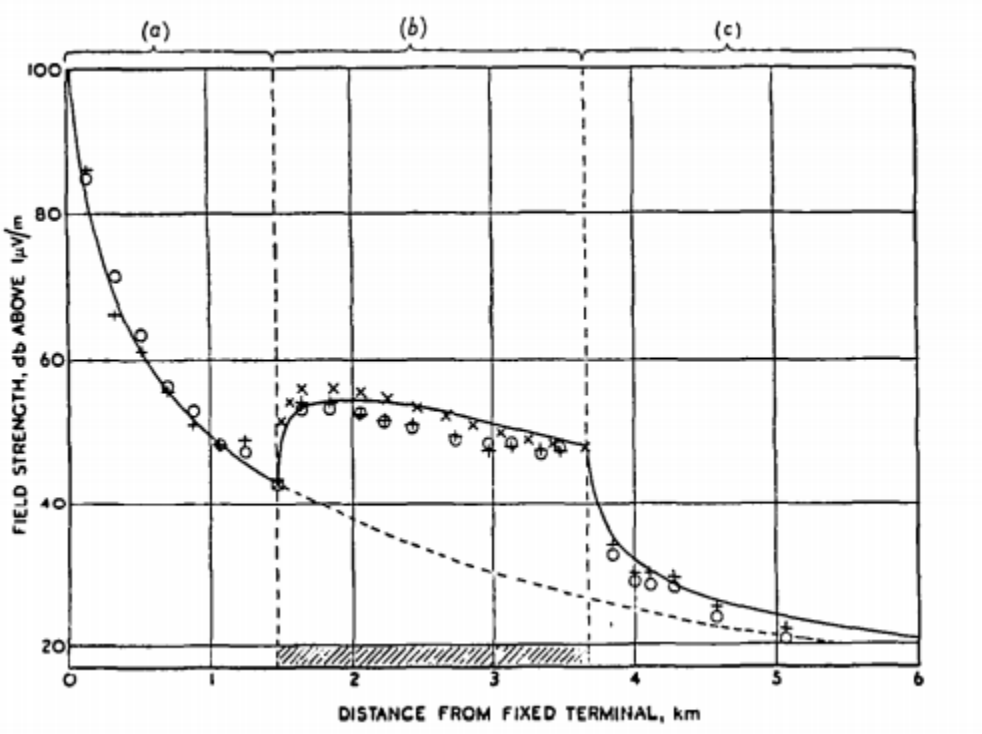

Figure 6 - Theoretical curve (solid) and experimental results for a land-sea-land path, as predicted by Millington [19]

LORAN relies on hyperbolic navigation techniques. A chain of LORAN stations work together to transmit a navigation pulse at a set interval. A chain is made up of at least 3 stations, operating in pairs, such that a triangulated fix can

be obtained. First, the master station of a chain sends its pulse, which is received by both the user and the slave stations of the chain. The slave stations wait a set amount of time, and transmit their respective pulses. Since the waiting times are known and strictly defined, the only delay which is unknown results from the signal's propagation time to the user [22].

Using this information, hyperbolic lines of position, or LOPs, can be drawn for any 2 LORAN stations operating in tandem. On any given line, the delay between receiving the 2 navigation pulses is constant. By using 2 sets of stations, the point at which the LOPs intersect can be determined as the point where the user is. Figure 7 demonstrates a graphical depiction of this process. The station located at M functions as the master, and X and Y serve as the slave stations.

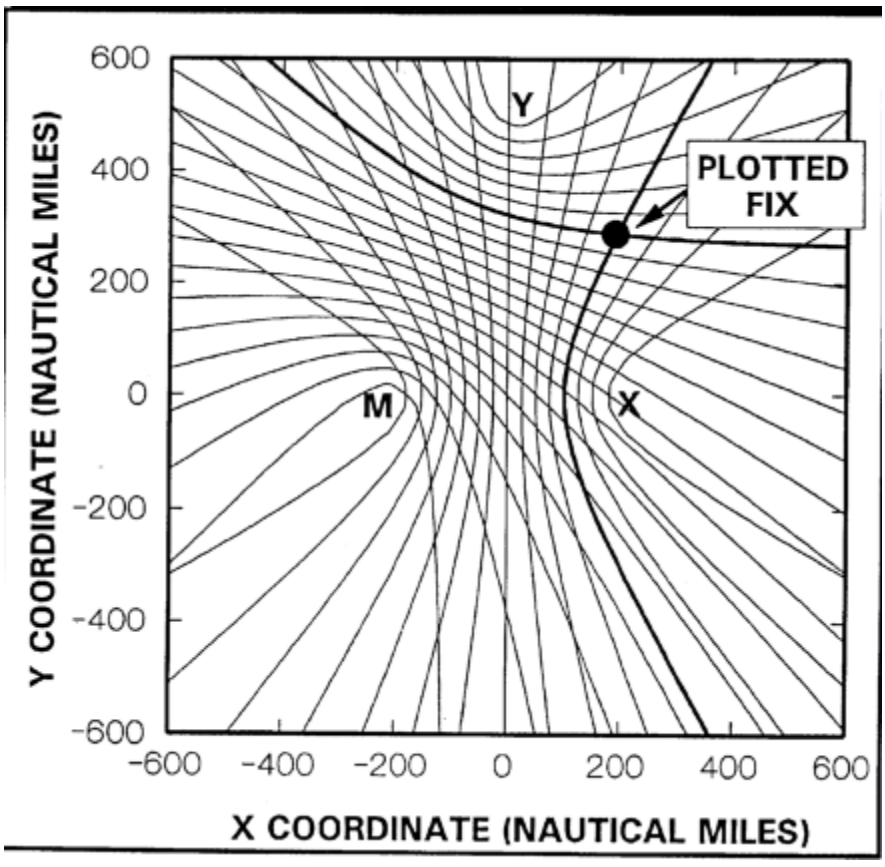

Figure 7 - LOPs depicting a master, 2 slave stations, and a plotted fix [22]

LORAN's primary usage has always been to sailors and aviators because the propagation phenomena over the irregular and inhomogeneous surface of land were not well understood during the time of its most widespread implementation. LORAN designers dealt with the delays of finite conductivity as phase factors. Since LORAN was designed to function over seawater, the variance in conductivities was only considered as a primary phase factor, a secondary phase factor, and an additional secondary factor (ASF) [22]. Millington's method was used directly to determine phase variances, and absolute accuracy better than 0.25 nautical miles was not strongly sought after. Figure 8 depicts the USCG table of phase factors and their explanations.

2.5: LORAN Propagation Modeling

Before the termination of the LORAN program in early 2010, LORAN was thought to be the single best choice to back up GPS. Its massive transmitted power, (on the order 0f 200 kW to 2MW) land based transmitters, capitalized infrastructure, and worldwide distribution make it an ideal candidate to back up GPS. To that end, numerous authors have conducted detailed studies of LORAN ASFs, how best to predict ASFs, and in general, how to increase LORAN's accuracy through propagation modeling.

One of the first authors to research LORAN propagation times was J. R. Johler [23] while his work was instructive, Johler's methods were completely experimental and not really predictive. He merely pointed out relatively large differences between predicted propagation velocities using standard methods and actual velocities based on results.

In 1952, Pressey et all [24] used the DECCA navigation system in great Brittan, coupled with Millington's method to predict the phase over a land path of mixed conductivities. Pressey's work was particularly instructive because of his care in outlining the path, demonstrating the total phase lag, and also the phase lag due only to changes in conductivity.

Quantity	Primary Phase Factor	Secondary Phase Factor	Additional Secondary Phase Factor
Abbreviation	PF	SF	ASF
Brief Description	A correction to a Loran-C reading due to signal propagation through the atmosphere as opposed to propagation through free space.	The amount, in usec, by which the predicted time difference of a pair of Loran-C signals that travel over all-seawater paths differs from that of signals that travel through the atmosphere.	The amount, in usec, by which the time difference of an actual pair of Loran-C signals that travel over terrain of various conductivities differs from that of signals which have been predicted on the basis of travel over all-seawater paths.
Function of	Atmospheric Index of Refraction	Conductivity and permittivity of seawater—time delay a function of distance.	Specific paths between master, secondary, and vessel.
Included on Loran-overprinted Charts	Yes	Yes	Yes, on nearly all charts, see chart legend for details
Included in Lat/Long Conversions on Loran-C Receivers	Yes	Yes	Yes, on most modern receivers, check owner's manual for individual set.
Additional Information Available From	See Glossary for details	See Glossary for details	See DMAHTC *Loran-C Correction Tables*, for various chains and secondaries.

Figure 8 - Table of phase factors used in LORAN calculations [22]

Some of the best time-domain representations of amplitude and phase error introduced by propagation over ground of finite conductivity were presented by Cooray in Radio Science [25]. He demonstrated that timing errors could be as high as 5 microseconds over a distance of several hundred kilometers. This error is equivalent to, or worse than, errors introduced by scattering from power line noise.

Without a doubt, the most authoritative study on LORAN ASFs, and the propagation model eventually used to predict propagation at ORNL was the work of Paul Williams, David Last, and those who followed in their footsteps. Williams and Last, while working at the University of Wales in Bangor, UK, utilized Monteath's compensation theorem [26] to predict ASFs for LORAN chains in Great Britain and Western Europe. In a series of 2 publications [27] [28], Williams and Last first modeled, and then measured ASF data for LORAN stations Vaerlandet, Ejde, and Slyt. Their results were a remarkable improvement over previous estimates using Millington's method.

Their model, programmed in C, became known as BALOR, (short for the BAngor LORan model). Having validated it, they began testing over longer distances, and discovered an erroneous "wobble" in their data. They were able to narrow the problem down to their model having an incomplete treatment of the spherical nature of the earth. Therefore, switching to Wait's derivations, which the reader will recall were covered earlier in the literature review, the modern day version of BALOR was arrived at. BALOR has been employed extensively by researchers at Ohio University, and from a publication by Blazyk and Diggle [29], the formulation of the ORNL propagation model has been created. Encapsulated within the ORNL formulation of BALOR are the effects of the finite conductivity on the ORNL range, and the irregularity of the terrain.

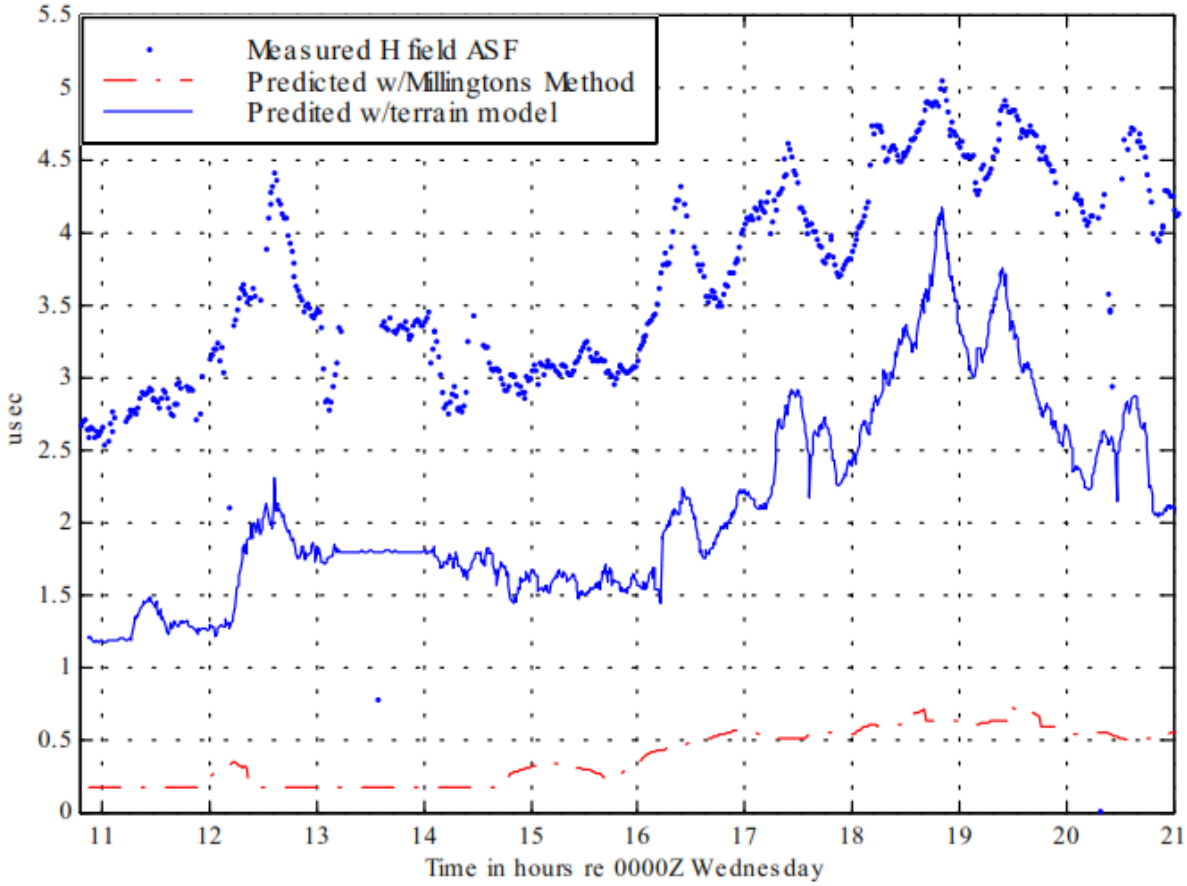

Figure 9 - Predicted and measured H field Additional Secondary Factor for LORAN station Ejde using BALOR and Millington's Method [28]

2.6: Forest Propagation Considered

Of additional concern is the dense forest over which the TPS signals are propagating. As such, the second portion of the literature review will be devoted to the study of forest propagation publications. While there are many publications on the subject, most deal simply with path loss in a forest environment. Most are not attempting to view the forest as a phase shifter. Since simple coverage predictions and calculations and the reception of AM and FM signals do not

require precise synchronization, most, if not all authors disregard the phase delay associated with forest propagation. However, based on their models, it is both instructive and important to attempt to extract a value for relative permittivity which fits with accepted theory.

First, how is the transmitted wave predicted to propagate through the forest canopy? Theodor Tamir [30] predicted that the air/treetop interface will guide the propagating wave much as the air/ground interface guides the ground wave. In fact, he was able to prove this by examining path loss for antennas deep in a foliage canopy. His first observation was that additional path loss due to vegetation was basically a constant over long, smooth propagation paths. Next, he observed that the additional loss varied significantly when either transmitting or receiving antenna was raised up above the canopy. Thus, Tamir postulated that the forest behaved as a lossy, dielectric slab with the air/canopy interface serving as the guiding medium.

Tamir's model is shown graphically in figure 10. It is important to note that on the ORNL range, only the lateral wave is of concern. The direct and reflected waves are attenuated beyond the point of being received, and due to the DSSS waveform, the sky-wave will arrive too late to be correlated by the receiver, and additionally, will arrive back at the earth's surface far beyond the point of the receiver. .

While this certainly seems plausible for smoothly varying terrain, Tamir qualifies his theory of treetop guidance in his conclusions by stating that the mechanism should hold for terrain of a certain smoothness.. The model proposed herein is that the treetop mode of propagation will hold, except in the case of extreme roughness in the terrain. Based on the assumption that the wave is weakly guided by the forest/air interface, the lateral wave may often penetrate the forest canopy, producing the effective velocity factor which is thought to exist. Therefore, since flat terrain is basically nonexistent on the ORNL propagation range, the velocity factor should be applied over all non-smooth sections of the paths.

The slab model is used extensively throughout literature for propagation in the 1-100 MHz region of operation, and it is safe to say that, for signals whose wavelength is large compared to the size of individual leaves and branches, (i.e. well into the GHz range) the dominant mode of propagation is the lateral wave.

Having confirmed the lateral wave to be the primary factor in determining propagation through the vegetation on the ORNL reservation, the final determination to be made relates to the acceptable range of relative permittivity which can be used and accepted as scientifically valid. After all, any velocity factor could be applied since this is a simple linear factor and only the endpoints of the data are of concern. However, it is important to remain scientifically rigorous, and choose values of relative permittivity which correlate with measured values.

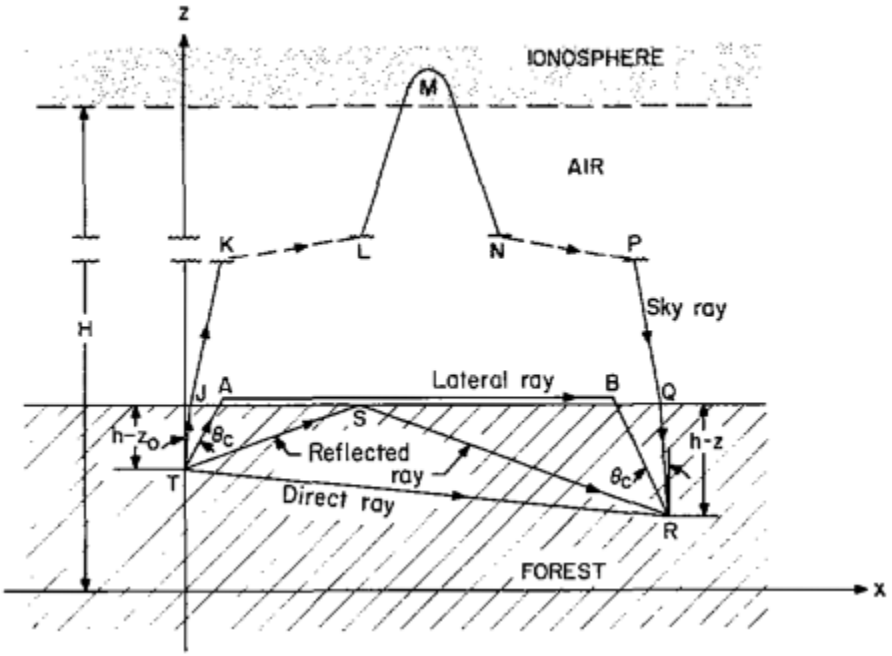

Figure 10 - Tamir's slab model for forest propagation [30]

First, the work of Parker and Makarabhiromya [31] is extremely instructive. Utilizing several different types of open wire transmission lines over 5 different

sites in Thailand, they were able to measure relative permittivity of vegetation. They studied both ground and vegetation characteristics and found forest relative permittivity to be on the order of .9 to 1.2. The relative permittivity less than unity can be caused by extremely favorable stem orientation such as that of an orchard or windbreak. These types of configurations can produce a wave guiding mode with some phase advancing properties. However, this type of situation is hardly relevant in natural growth due to its random distribution Tamir [30] utilized relative permittivity ranging from 1.01 to 1.5 in an effort to be exhaustive. However, further examination of the literature proves this much of a range to be far larger than necessary.

In a much later MILCOM publication, Le Palud [32] compares results with Tamir's theories but utilize a Parabolic Equation formulation and computer modeling. Their study found the forest permittivity to fall well within the limits of Parker and Makarabhiromya, sitting at a nominal value of 1.06.While results outside of the forest differed in large ways at times, the authors observed strong similarities inside of the forest, and attribute the discrepancies at forest borders to Tamir's simplifications of diffraction phenomena.

Another model considered by the Defense Research Corporation [33] also utilized a dielectric slab approximation. Once again, the data utilized was obtained from jungles in Thailand, with an average permittivity of 1.02 assumed. The experimental data utilized vertically polarized antennas located within the forest canopy, much like Tamir's original experiments.

Finally, following on the heels of his original work, Tamir published another work in conjunction with Dence, studying the loss mechanisms of a lateral wave in forested environment. Here, Tamir finds the thin forest characteristic permittivity to be on average, approximately 1.03 and the average forest permittivity to be on the order of 1.1 [34]. Thus, his earlier assumptions of 1.01 to 1.5 were extremely exhaustive.

Having studied extensively the effects of finite conductivity, irregular terrain, and forestation on the propagation characteristics of the ground wave, it

is possible to begin constructing the mathematics which will be utilized to evaluate the endpoints of the propagation paths at ORNL. First the conductivity model from the BALOR literature will be developed using a modified flat earth solution. The distances of propagation involved are well within the parameters of expected validity for a modified flat earth solution, next, the irregular terrain assumptions, will be added. Finally, the forest propagation model will be added to complete the predicted delay profiles.

3: MATERIALS AND METHODS

At the heart of GPS and TPS operation is a simple, linear, algebraic equation.

$$\boldsymbol{d = rt} \tag{3.1}$$

Given a point in 2 or 3 dimensional space, and knowing the location of a radio transmitter precisely, a software algorithm can easily derive a position or fix, based on the transit times of the signals to the user. Each satellite or transmitter sends out a time stamped navigation message containing its location and the time of sending. Based on this information, a sphere can be constructed in 3 dimensional space, and based on the time offset and the speed of light, the user is determined, or fixed, to be on the surface of a sphere that has a radius equal to the speed of light times distance. When 3 or more of these spheres intersect, the user's position can be precisely defined.

There is, of course, a problem with this methodology. EM radiation does not move with a fixed velocity except in a vacuum, and therefore the actual distance travelled is an unknown. With GPS, propagation estimates are slightly easier, as the Ionospheric medium is, relative to that of a ground wave, fairly homogeneous. With TPS however, much more care must be taken to effectively predict the actual velocity of propagation versus the theoretical datum. There are several effects which perturb the phase of the propagating ground wave. The first effect which will be mathematically derived is that of the finite conductivity, spherical nature, and irregularity of the earth. These will be combined into a single derivation, as they are most often studied together.

3.1: Effects of Finite Conductivity and Irregularity of Terrain

At the heart of the ground wave propagation problem is to solve for the mutual impedance between transmitter and receiver terminals. This can be

approximated to within extremely accurate error bounds by an integral equation over the surface of the earth from the transmitter to the receiver [27].
The general approach is to find an attenuation function, *W* such that:

$$W = \frac{E_R}{E_0} \tag{3.2}$$

Where E_R is the actual received field, and E_0 is the received field of a vertically polarized transmitting antenna at the same distance. The latter value is well known [35]. Consider the situation shown in figure 11.

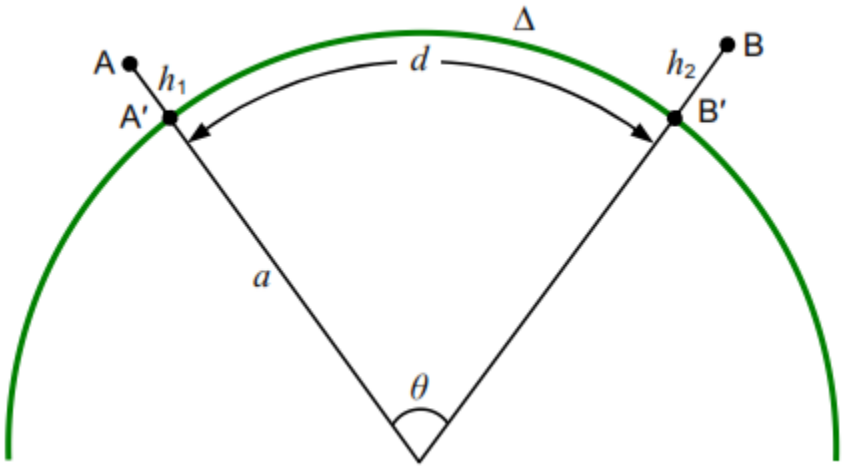

Figure 11 - Propagation over a smooth, homogeneous earth [29]

When the transmitter heights of A and B are sufficiently small, the integral equation can be expressed in terms of a residue series, and the attenuation function, *W* found as

$$W = e^{\left(\frac{-j\pi}{4}\right)}\sqrt{\pi x}\sum_{s=1}^{\infty}\frac{e^{(-j\pi t_s)}}{t_s - q^2} \tag{3.3}$$

$$x = A\theta \tag{3.4}$$

$$q = -jA\Delta, \tag{3.5}$$

$$A = \left(\frac{k_0 a}{2}\right)^{\frac{1}{3}} \tag{3.6}$$

$$\theta = \frac{d}{a} \tag{3.7}$$

Δ, the normalized surface impedance, is described as:

$$\Delta = \left(\frac{k_0}{k_1}\right)\sqrt{1 - \left(\frac{k_0}{k_1}\right)^2} \tag{3.8}$$

With

$$k_0 = \omega\sqrt{\mu_0 \varepsilon_0} \tag{3.9}$$

$$k_1 = \sqrt{-j\omega\mu_0(\sigma_1 + j\omega\varepsilon_1)} \tag{3.10}$$

When expressed in this manner, the roots t_s are complex roots of the differential equation.

$$w_1'(t) - qw_1(t) = 0 \tag{3.11}$$

When dealing with a physical propagation situation, equation 3.11 must be differentiated again to obtain

$$\frac{dt_s(q)}{dq} = \frac{1}{t_s(q) - q^2} \tag{3.12}$$

Then, for small values of q, the Taylor series expansion

$$t_s(q) = \sum a_n q^n \tag{3.13}$$

Must be used with

$$a_0 = t_s^0 \tag{3.14}$$

$$a_n = \frac{1}{n!} \frac{d^n[t_s(q)]}{dq^n}\bigg|_{q=0} \tag{3.15}$$

Following the application of Newton's method, the values of t_s can finally be extracted, but to call the process, described fully in [36], involved is an understatement. Particularly when the measured range is less than $(5\lambda_{0m})^{1/3}(km)$, as specified by [36] the residue series can take hundreds of terms to converge. Since every path at ORNL meets this criterion, it is best to formulate a more convergent method of determining *W.* Therefore, a small curvature, modified flat earth series will be used to describe *W*, instead of the residue series.

The small curvature formula was first described in [18], and is most applicable to transmitters and receivers placed such that their height compared to wavelength is minimal. This is precisely the case at the ORNL range, where the transmitting and receiving antennas are within 10 m of the ground. This formulation is taken from [36] and is described thus:

$$W = 2\sum_{m=0}^{10} A_m\left[e^{(j\pi/4)}qx^{1/2}\right]^m \quad 3.16$$

In the small curvature formula, $x, q, A, \theta,$ and Δ retain the values specified in equations 3.4-3.8, respectively. The terms of A_m, which are arranged in increasing powers of q, are listed in both [36] and [29], and are written directly as\

$$A_0 = 1 \quad 3.17$$

$$A_1 = -j\sqrt{\pi} \quad 3.18$$

$$A_2 = -2 \quad 3.19$$

$$A_3 = j\sqrt{\pi}\left(1 + \frac{1}{4q^3}\right) \quad 3.20$$

$$A_4 = \frac{4}{3}\left(1 + \frac{1}{2q^3}\right) \quad 3.21$$

$$A_5 = -\frac{j\sqrt{\pi}}{2}\left(1 + \frac{3}{4q^3}\right) \quad 3.22$$

$$A_6 = -\frac{8}{15}\left(1 + \frac{1}{q^3} + \frac{7}{32q^6}\right) \quad 3.23$$

$$A_7 = \frac{j\sqrt{\pi}}{6}\left(1 + \frac{5}{4q^3} + \frac{1}{2q^6}\right) \quad 3.24$$

$$A_8 = \frac{16}{105}\left(1 + \frac{3}{2q^3} + \frac{27}{32q^6}\right) \quad 3.25$$

$$A_9 = -\frac{j\sqrt{\pi}}{24}\left(1 + \frac{7}{4q^3} + \frac{5}{4q^6} + \frac{21}{64q^9}\right) \quad 3.26$$

$$A_{10} = -\left(\frac{32}{945} + \frac{64}{4q^3} + \frac{11}{189q^6} + \frac{7}{270q^9}\right) \quad 3.27$$

As a figure of merit, figure 12 compares the residue series, flat earth series, and the small curvature, modified flat earth series. It is clear that for short distances, the small curvature formula is extremely accurate, if not indistinguishable from the residue series.

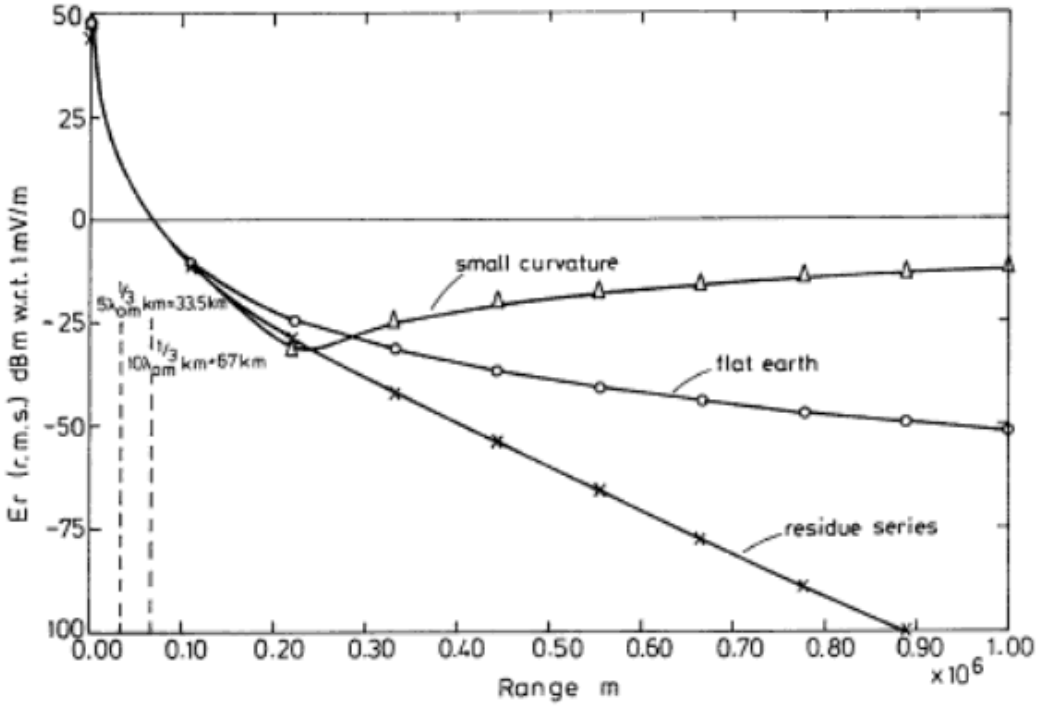

Figure 12 - Comparison of small curvature, flat earth, and residue series attenuation functions [36]

The power series expansion could be continued to higher order coefficients, but authors consider the first 11 terms to be an acceptable level of

accuracy out to the range at which the residue series begins to converge. Nowhere in literature is a larger number of coefficients directly available.

The assumed conductivity for the earth's surface is 1 mS/m, based on FCC conductivity maps depicted in figure 12. While the entire Tennessee valley is assumed to be 2 mS/m, those familiar with the topology apply that figure to the fertile and well watered bottom lands of the valley, particularly areas close to the Tennessee River. With the ORNL area being very hilly, much rockier, and unsuitable for farmland, a better estimate for conductivity is 1 mS/m.

Having completed the development of the conductivity model for a smooth earth, the next step in the derivation is to account for irregular terrain. Irregular terrain is defined as changes in elevation not related to the spherical characteristics of the earth. The surface impedance will be replaced by the following:

$$\Delta_e = -\frac{E_{\theta 2}}{Z_0 H_{\phi 2}} \cos\alpha + \frac{E_{r2}}{Z_0 H_{\phi 2}} \sin\alpha \qquad 3.28$$

Where α is the slope angle between adjacent terrain points. For distances in the far field however, there is a simpler approximation which is acceptable.

$$\Delta_e = \Delta \cos\alpha - \sin\alpha \qquad 3.29$$

The slope angle between adjacent points was found by first taking the length of the entire path and dividing by the number of DTED points, thus giving the path interval. This value is assumed to be the "run" between points. The "rise" is easily found as the elevation change between points. Thus, the slope angle between points can be found as the arctangent of these two values, as illustrated in figure 14.

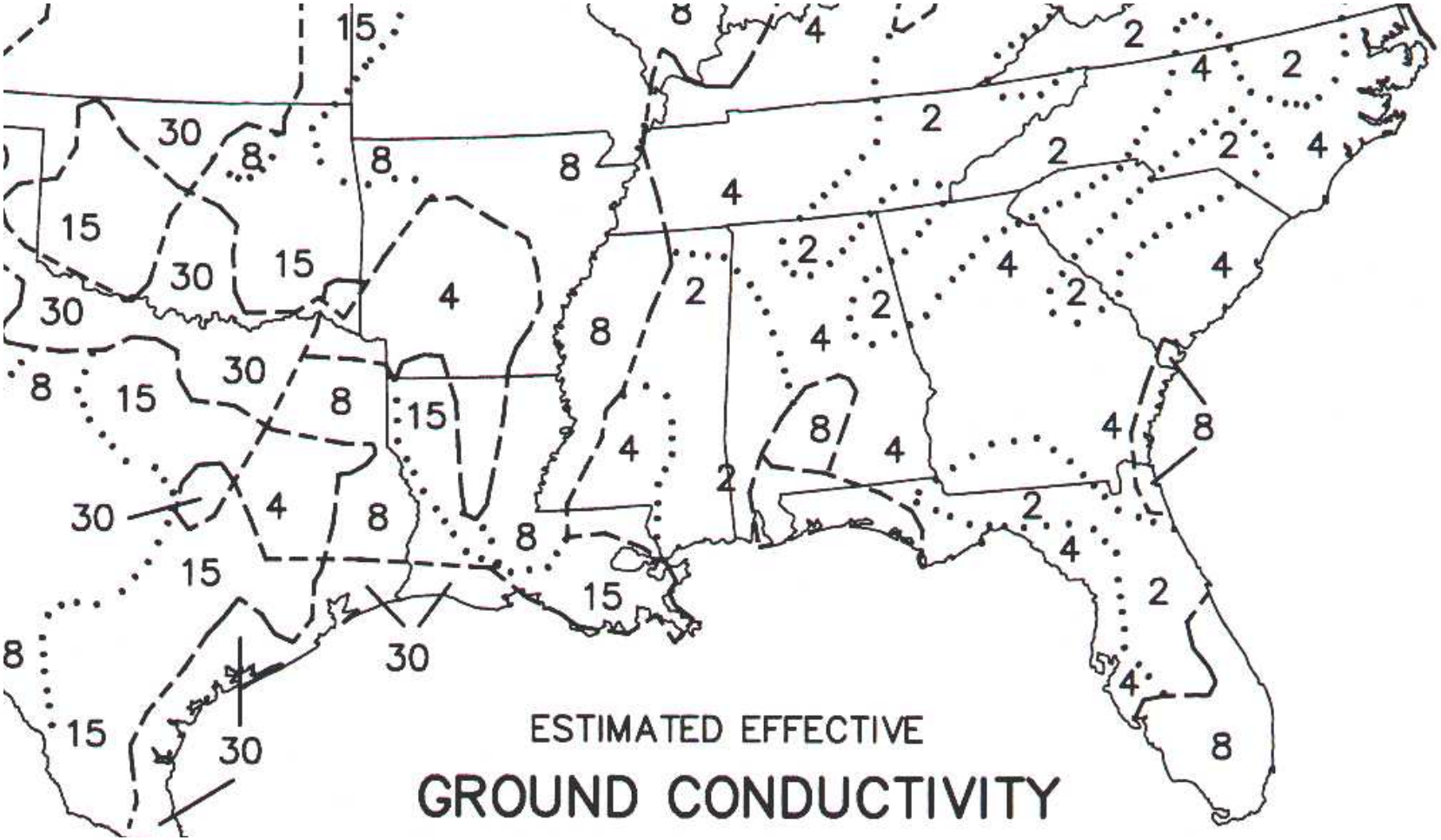

Figure 13 - Ground conductivity map for the Southeastern Continental United States [37]

In order to prevent excessive noise introduced by the sharply varying terrain, and exacerbated by the quantized nature of the 9 meter resolution of the DTED databases, a rectangular moving average filter was applied to the elevation profiles before calculating the impedance perturbation. Figures depicting both the smoothed and unsmoothed profiles are available in appendix A.

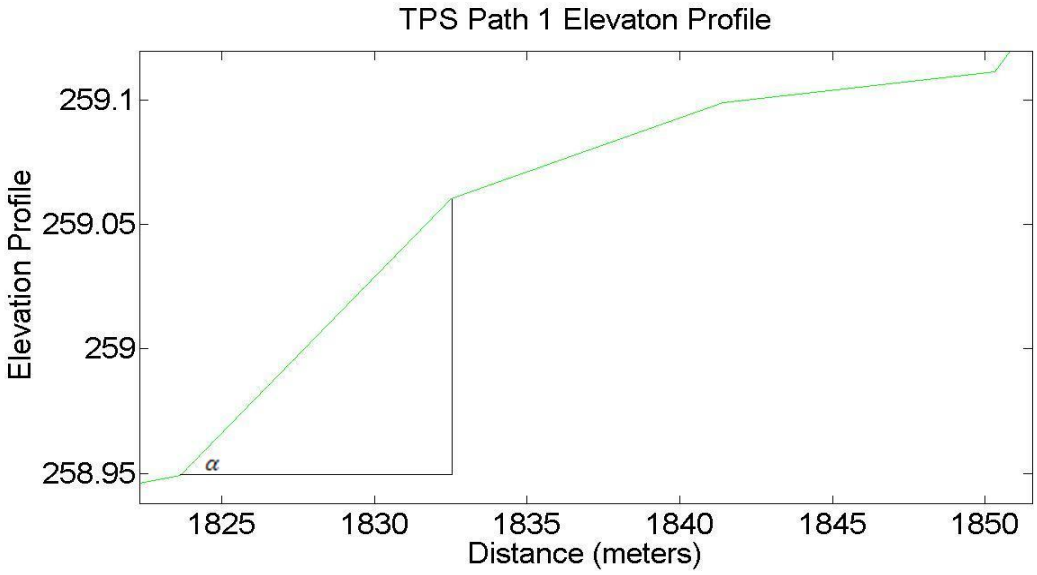

Figure 14 - Slope of angle calculation illustration

Thus, having completed slope angle calculations, the finite conductivity and irregular terrain modeling is complete. The algorithm returns the result in radians, and thus to convert to seconds of delay, one need only divide by the radian frequency. Next, the forest propagation model needs to be developed.

3.2: Forest Propagation Model Development

Since the introduction of Theodore Tamir's theories in 1967, one of the most popular models to represent propagation through a forest medium has been the dielectric slab model. As explained in the literature, the slab model characterizes the forest as a homogeneous medium with a conductivity and

permittivity of its own, and the earth/air interface guides a lateral wave over the treetops. However, no literature exists to support the claim that this waveguide mechanism takes place in terrain that is not smoothly varying. As such, a modification of this theory is put forth herein. It is postulated that the lateral wave is only weakly guided by the air/forest interface, and that, as a result, the wave exits and reenters the forest canopy throughout its journey from transmitter to receiver.

Since the wave spends a significant amount of time within the forest canopy, it is appropriate to apply a velocity factor [38] such that the velocity of the wave is reduced. The new velocity can be described as

$$V_{forest} = V_{air} \frac{1}{\sqrt{\varepsilon_r}} \tag{3.30}$$

While some may question the use of a simple linear scale factor in order to correct for such a non-linear problem, particularly in a situation where data is simply being fitted, questions of data cooking are easily avoided by returning to literature. As stated in the literature review, measured and estimated relative permittivity has been found in several sources. Table 2 summarizes sources, propagation mediums, and relative permittivity found by several authors, in addition to the data utilized to predict propagation times on the ORNL range. As can be observed from the table, the values necessary to acceptably fit the data at ORNL fall easily within the limits found by all authors who have attempted to characterize forest in this way. Thus, it is safe to say that this is a valid extension of the dielectric slab model.

The level of forestation had to be determined manually. This was done utilizing satellite imagery obtained from Google© Earth. First, each transmitter and receiver was precisely marked using the place mark feature. Figure 4 shows this arrangement. Next, the ruler function was used to measure each type of forest. Whenever there was a significant change in the level of forestation, a new velocity factor was assigned and a new measurement began. Examples of the

two levels of forestation are shown in figure 15, and an example of distance measurement is shown in figure 16.

Table 2 - Comparison of literature relative permittivity and those found for ORNL reservation

Source	Medium	Range of ε_r
Parker and Makarabhiromya [31]	Jungle	1.01-1.2
Le Palud [32]	Forest	1.06
Defense Research Corporation [33]	Jungle	1.02
Tamir and Dence [34]	Varied Forest	1.03-1.1
ORNL Range	Thin Forest	1.03.1.05
ORNL Range	Thick Forest	1.07-1.1

Figure 15 - Comparison of thin forest (top) and thick forest (bottom) as determined by satellite imagery

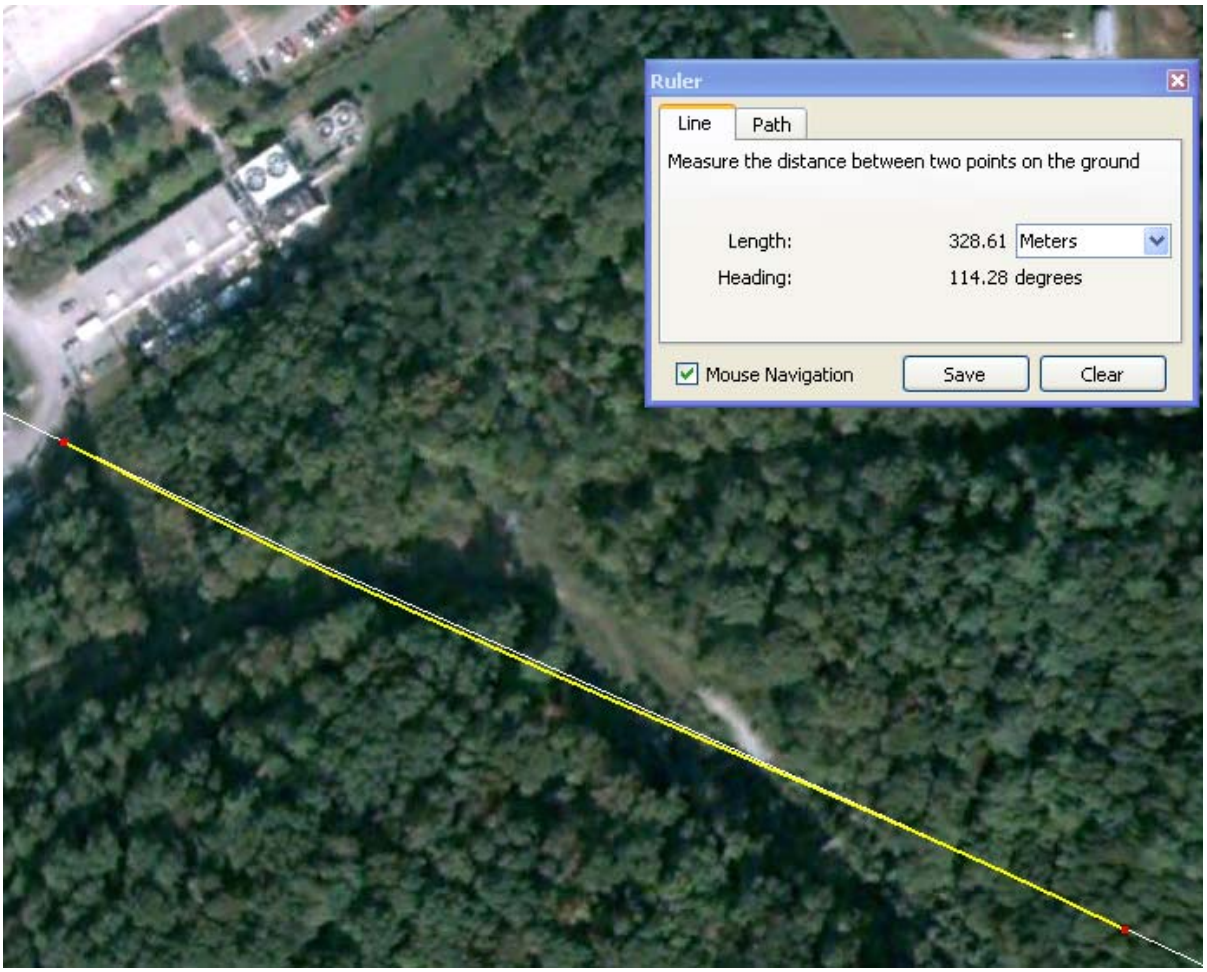

Figure 16 - Measuring the length of a section of thick forest. A transition to open ground is just visible at the left edge of the figure

Using the relative permittivity ranges listed in table 2, the appropriate velocity factors were applied along the paths on the ORNL range, and the estimated propagation delay compensation was adjusted to reflect the new predictions. Figures 17-21 demonstrate the complete delay profile moving from transmitter to receiver along paths 1-5.

Along paths 2 and 3, the phase nearly matches that of the forest propagation delay, but in the cases of paths 1, 4 and 5, there is significant deviation due to terrain roughness.

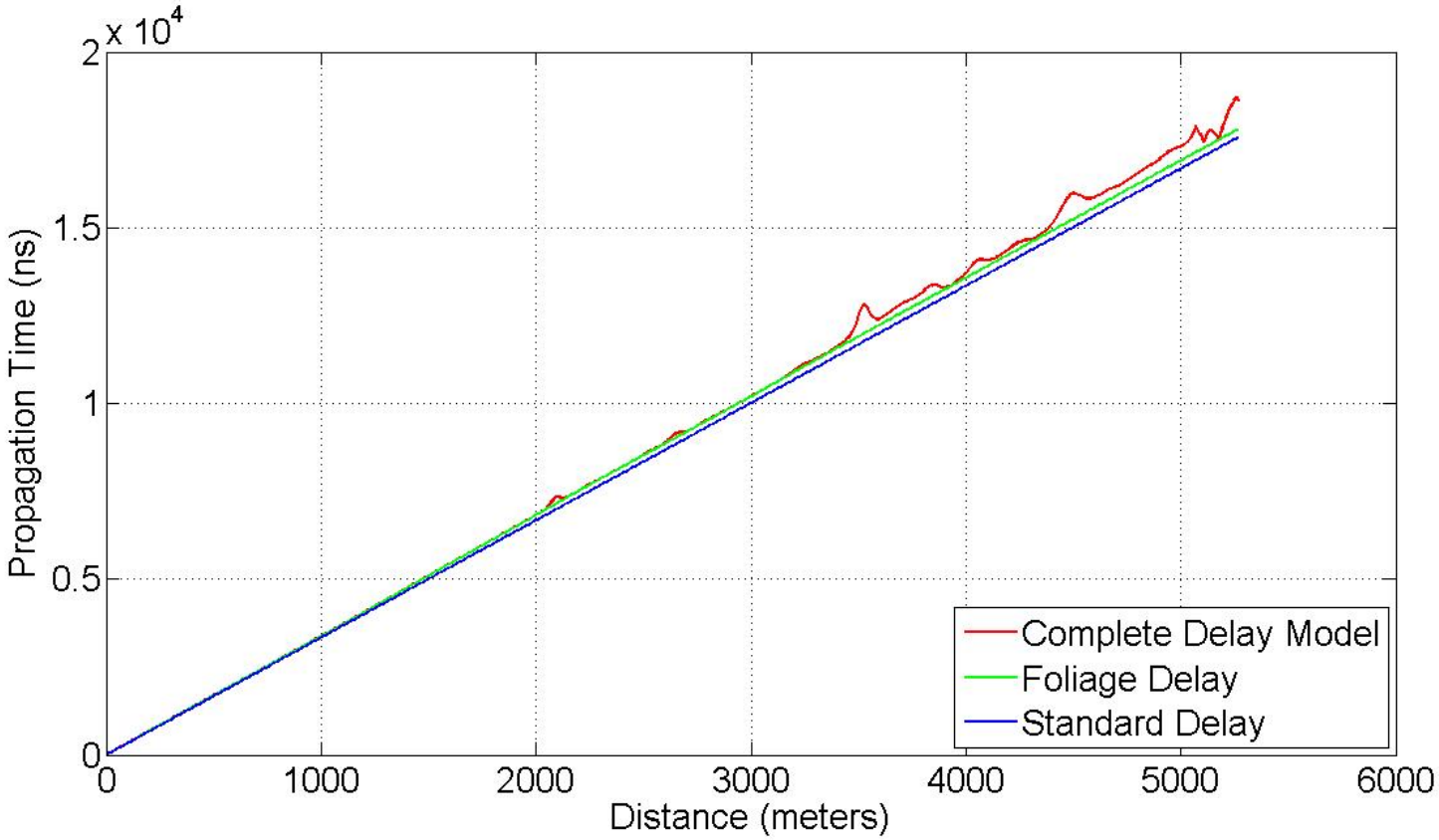

Figure 17 - Delay profile for path 1 depicting standard delay of 1.0171 ns/ft, delay associated with only forest velocity factor, and delay associated with forest propagation, finite conductivity, and irregular terrain

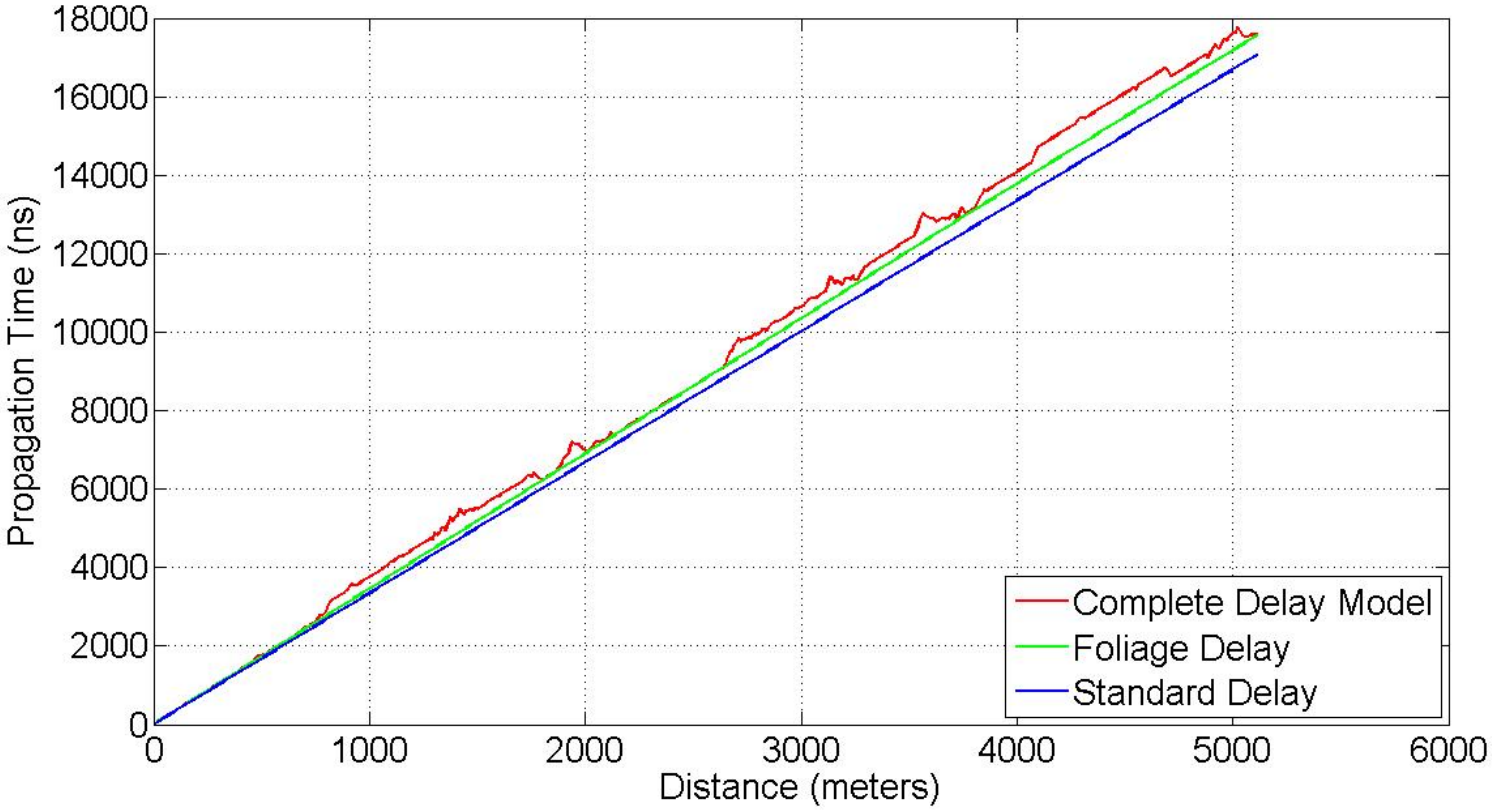

Figure 18 - Delay profile for path 2 depicting standard delay of 1.0171 ns/ft, delay associated with only forest velocity factor, and delay associated with forest propagation, finite conductivity, and irregular terrain

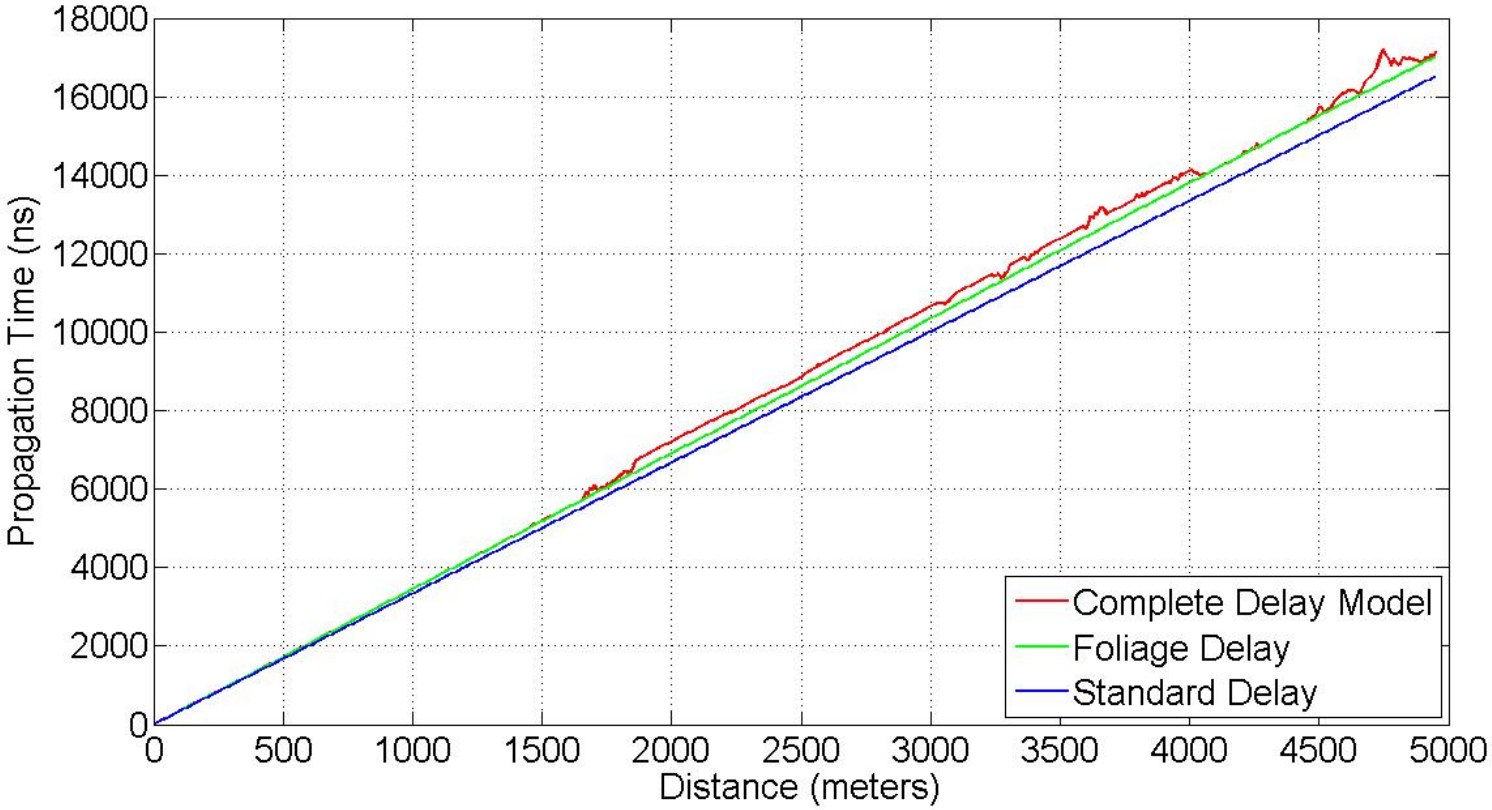

Figure 19 - Delay profile for path 3 depicting standard delay of 1.0171 ns/ft, delay associated with only forest velocity factor, and delay associated with forest propagation, finite conductivity, and irregular terrain

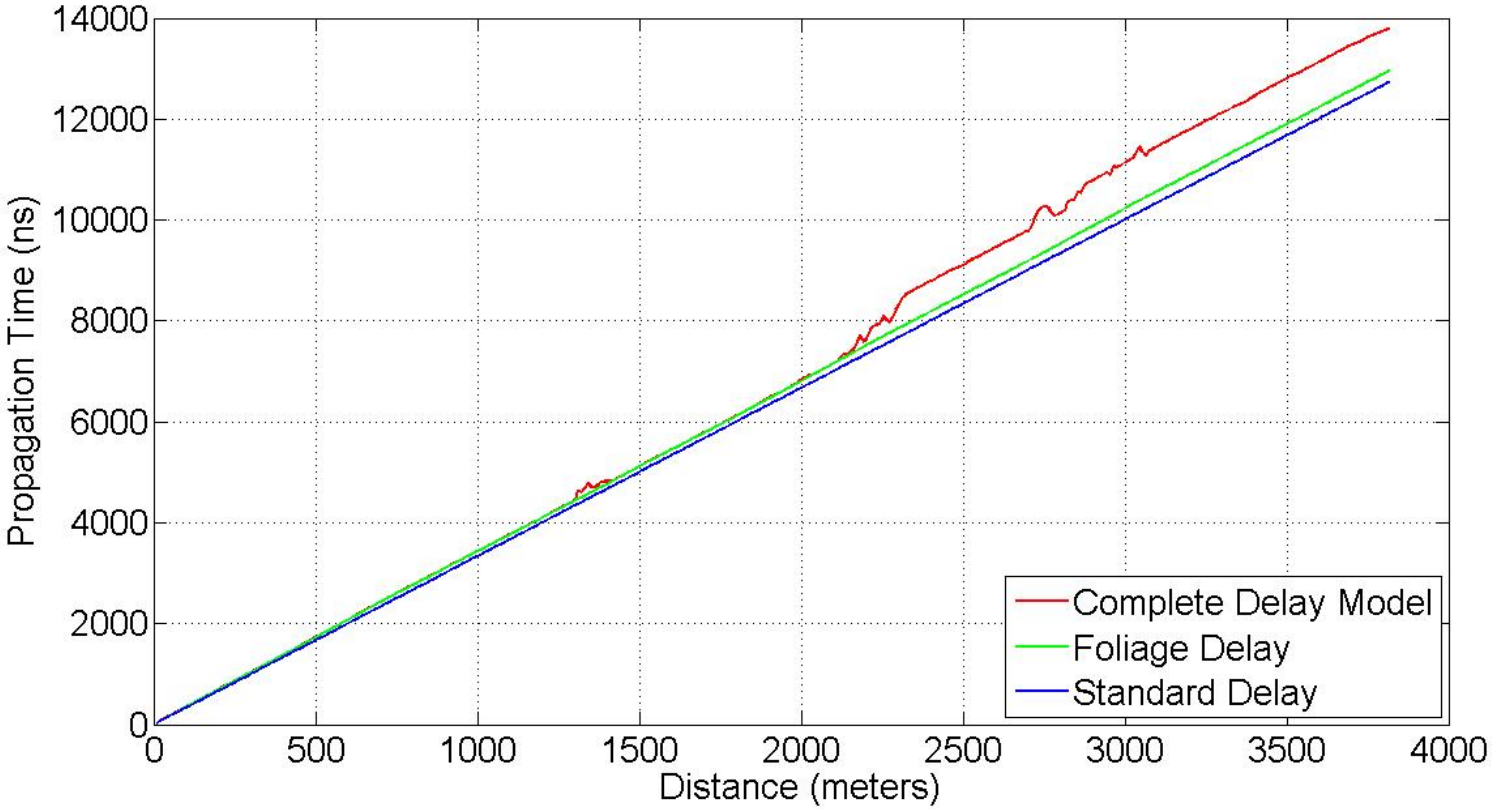

Figure 20 - Delay profile for path 4 depicting standard delay of 1.0171 ns/ft, delay associated with only forest velocity factor, and delay associated with forest propagation, finite conductivity, and irregular terrain

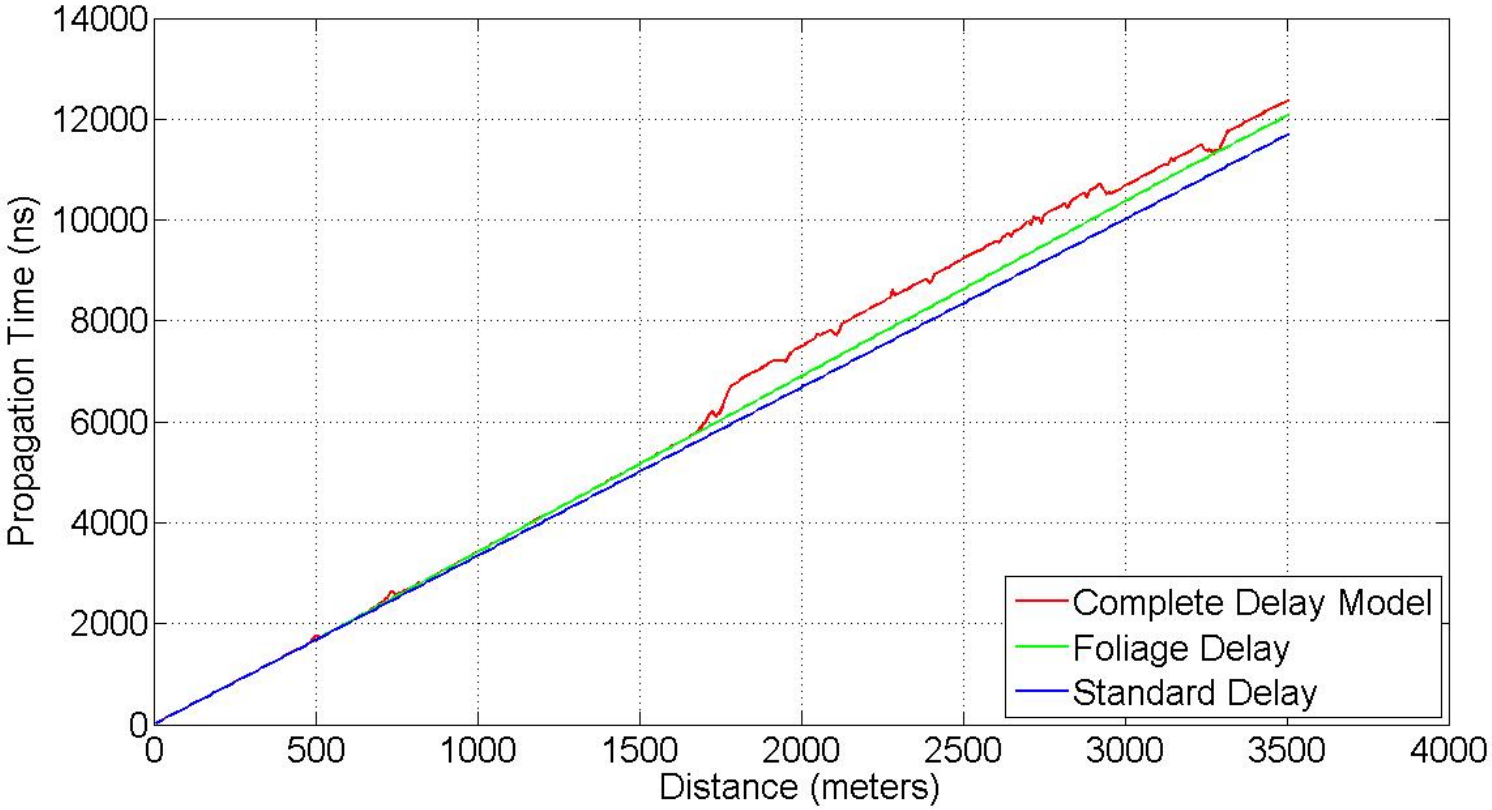

Figure 21 - Delay profile for path 5 depicting standard delay of 1.0171 ns/ft, delay associated with only forest velocity factor, and delay associated with forest propagation, finite conductivity, and irregular terrain

Even in the case where the forest propagation factor is the primary contributor to the endpoint, this is effectively predicted by the irregular terrain model. Having completed a survey of the methods used and predictions, the time has come to discuss the model's effectiveness at predicting the time of arrival of the propagated wave.

4: RESULTS AND DISCUSSION

The model's results must be discussed in several contexts. While its accuracy is the primary figure of merit, it is also important to consider ease of implementation in embedded hardware and expansion to include other effects.

4.1 Accuracy

The tabulated results of paths 1-5 are shown in table 3. The model showed never before seen levels of accuracy at predicting the phase of the ground wave over short distances, with maximum ranging error along any path being 26 ns. Note that because the formula used to measure the discrepancy between measured and predicted pseudo ranges is:

$$discrepancy = estimated - measured \qquad 4.1$$

A negative number in the discrepancy column corresponds to a prediction which is too short, while a positive number corresponds to a prediction which is too long. In addition to the tabulated data in table 3, figure 21 shows (roughly) the physical locations which the predicted ranges correspond to, assuming that the error lies in a straight line connecting the transmitter and the receiver. This figure is zoomed in to show the detail around the receiver site.

As is clear from figure 22, all pseudo ranges place the location of the receiver antenna on top of the building, within 25 feet of its actual location. Figure 23 shows the initial pseudoranges relative to the final predicted pseudoranges. Over short distances, in forested and irregular terrain, the model developed for predicting propagation at ORNL has shown itself to be successful. Using only a single GPS fix for each of 5 transmitters located around a central TPS receiver, correct pseudo ranges have been calculated to within 26 ns over distances not less than 2 miles.

Utilizing this method, it should be possible to locate a dismounted soldier or other asset within a building, intersection, or similarly sized feature of interest, despite a lack of GPS service.

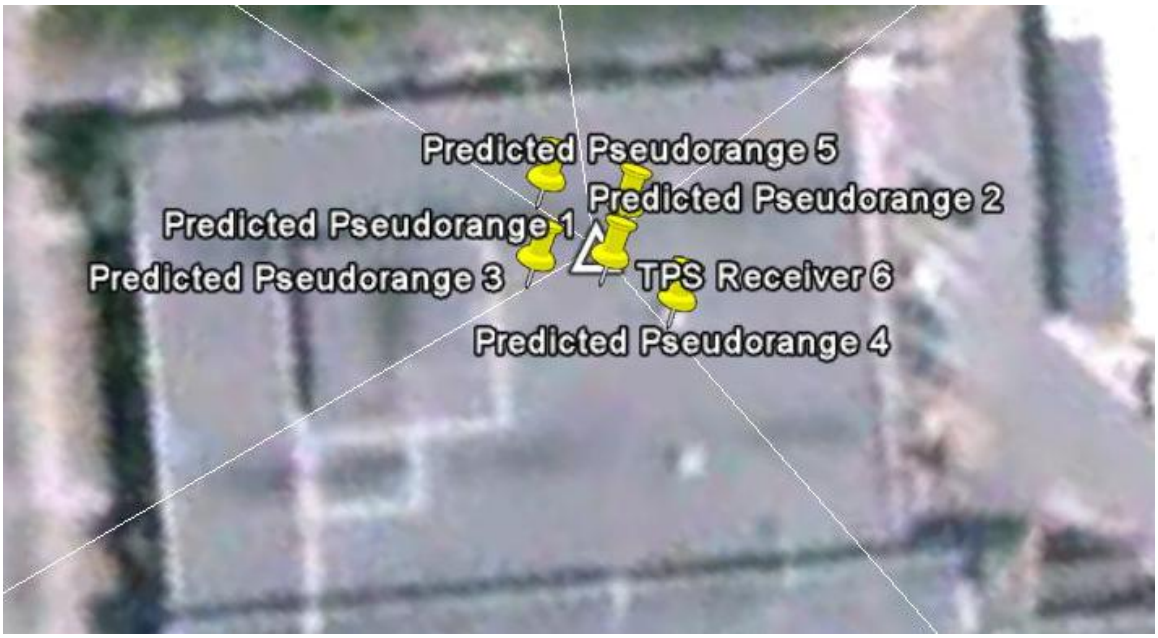

Figure 22 - Graphical depiction of final predicted pseudorange locations

Table 3 – Observed propagation times on ORNL range, along with discrepancies between predicted and actual propagation times after applying the theories discussed herein

Xmit Position ID	Recv Position ID	Smoothed Path Delay (ns)	Propagation Correction	Total Est. Delay (ns)	Thin Forest Relative Permittivity	Thick Forest Relative Permittivity	Measured Pseudo-range (ns)	Difference [Est. - Meas.] (ns)
1	6	17573.31	1034.4	19638.71	1.03	1.08	19631.237	7.4733758
2	6	17070.47	520.091	18871.56	1.03	1.07	18889.237	-17.679371
3	6	16512.37	699.1405	18492.51	1.03	1.08	18448.237	19.289945
4	6	12730.51	1066.3	14827.81	1.05	1.1	14854.237	-26.428975
5	6	11701.41	663.0038	13395.42	1.04	1.09	13401.237	-5.8195697

Figure 23 - Approximate physical locations of initial pseudoranges relative to TPS receiver site 6, compared to the final predicted pseudoranges

4.2 Ease of Implementation

Knowing that the time of arrival for an EM wave can be predicted using such simple algorithms as a linear scale factor and trigonometric functions provides great flexibility for future implementations of the algorithm. Such simple algorithms prove relatively easy to implement in a platform which can be placed in the hands of a dismounted soldier or built into a civilian GPS receiver. Without having to make complicated models, store large lookup tables, or run complex EM software, a reliable result can be obtained and delivered to the end user quickly. This is of particular note due to the stringent constraints often placed on embedded systems for civilian and military applications. No matter how accurate a given technology is, if it cannot meet SWAP requirements, it will never be effectively utilized. Due to the relatively simple algorithm used in this model, it is safe to say that it could be easily utilized in an embedded context.

4.3 Use of Superposition

It is also noteworthy that the creation of this model involved a mathematical description of the effects which allowed for superposition of two previously unrelated phenomena. This opens up the model to be expanded in the future, possibly to account for urban environments or other, as yet undetermined, effects, so long as future model components continue to utilize the same method of superposition.

5: CONCLUSIONS AND RECOMMENDATIONS

While the propagation model has shown itself to be successful in its first 5 trails, there are several rounds of additional testing and automation which it will need to undergo in order to be fully prepared for automated operation.

5.1 Large Scale Testing

First, and perhaps most importantly, the model must be tested over much longer distances to ensure that its error does not increase significantly as a function of distance. While the original trials are very promising, any ground wave based system will require ground wave propagation over thousands of miles, not dozens. If positioning error is found to increase linearly as a function of distance, this model of propagation prediction will be useless within dozens, not thousands, of miles. While the ideal solution would have been to test more extensively before publicizing results, the cost of installing such a capital-intensive testing range prevented the gathering of longer-range data.

5.2 Automation of Forestation Determination

Next, the prediction algorithm's forestation determination must be automated. Currently, an operator must manually examine satellite imagery to determine the level of forestation present over a given path. This takes an inordinately large amount of time (10-15 minutes per path, even for distances of only 2-3 miles) and is somewhat subjective. This process could be automated in one of two ways: either through the use of image recognition software to scan and determine forested areas, or by the use of a global database. Unfortunately, neither of these options is currently reduced to practice, although the latter would appear to be closer to realization than the former [39]. In addition to being the solution which is closer to implementation, an up-to-date global forestation database would not be subject to the nuances of image recognition such as shadowing effects and cloud cover. The major challenge of a forestation

database would be servicing and maintaining it in order to ensure positioning accuracy.

5.3 Consideration of Depolarization

Next, at least once during discussion of results, the question of depolarization of the signal has been discussed. Due to the horizontal orientation of most forest foliage, the currents which are induced in leaves and small twigs tend to severely depolarize vertically polarized EM waves [40]. However, no literature exists as to whether or not this depolarization seriously affects the perceived time of arrival of the propagated wave. The accuracy of prediction obtained over short distances would lead to the belief that it does not, but since the effect was not physically measured, it is difficult to discern whether significant depolarization has, in fact, occurred.

Since horizontal polarization is known to be more efficient in a forest environment in terms of path loss [40], operating the TPS system with horizontal polarization in heavily forested areas might be worth considering as a method for increasing available coverage area. This does, unfortunately, give rise to a lose-lose situation in terms of propagation efficiency. While horizontally polarized waves are known to propagate further in a strictly forested environment, vertically polarized waves are the method of choice for longer-range ground wave propagation due to their markedly better propagation efficiency over “normal” terrain.

5.4 Time Varying Model Development

Next, the propagation conditions are known to be time varying. Depending on the season and the corresponding forestation or lack thereof, a time difference of approximately 100 ns per path has been observed when making predictions. As one would expect, the heavy foliage of the late spring, summer, and early fall causes the delay to be markedly higher when the forests are in full canopy, as opposed to the winter, when significant deforestation occurs. An

automatic time variance factor should be taken into account during the final setup of a field-ready application. This could be accomplished in several ways, the most convenient being extraction of season based on the date, and an initial GPS fix. Using these two pieces of information, the season could easily be extrapolated, and thus the forestation roughly determined. Alternately, on-site radio engineers or end users could be instructed on how to make proper forest inspections to accurately determine the level of canopy. From these observations, base forest velocity factors could be applied.

LIST OF REFERENCES

[1] "National PNT Advisor Board commonts on Jamming the Global Positioning System - A National Security Threat: Recent Events and Potential Cures," International LORAN Association, 2010.

[2] "Global Positioning System Standard Positioning Service Signal Specification," The National Executive Committee for Space-Based Positioning, Navigation, and Timing , Washington D.C., 1995.

[3] John A. Volpe National Transportation Systems Center, "Vulnerability Assessment of the Transportation Infrastructure Relying on the Global Positioning System," U.S. Department of Transportation, 2001.

[4] Maj. William Wright, Michael Russel, and John Brockhaus, "Myth Busted: Civilian GPS Receivers Actually do Have Access to the L2 Frequency," *Army Space Journal*, vol. 9, no. 3, pp. 46-47, 2010/2011.

[5] P. Theerapatpaiboon, P. Supnithi, N. Leelaruji, and N Hemmakorn, "The Analysis of Ionospheric Scintillation on the Global Positioning System (GPS) at Bangkok," in *SICE-ICASE, 2006. International Joint Conference*, 2006, pp. 3632-3635.

[6] T Buck and G Sellick, "GPS RF Interference via a TV Signal," in *Proceedings of the 10th International Technical Meeting of the Satellite Division of the Institute of Navagation*, Kansas City, 1997.

[7] Terence Barrett, "History of Ultra Wideband Communications and Radar: Part 1, UWB Communications," *Microwave Journal*, vol. 44, no. 1, January 2001.

[8] P Ward, "GPS Receiver RF Interference Monitoring, Mitigation, and Analysis Techniques," *Navigation - Journal of the Institute of Navigation*, vol. 41, no. 4, Winter 1994.

[9] S Gilmore, "The Impact of Jamming on GPS," Volpe National Transportation Systems Center, Cambridge, MA, Symposium 1998.

[10] B., et al. Winer, "GPS Receiver Laboratory RFI Tests," in *Proceedings of the Institute of Navigation National Technical Meeting*, Santa Monica, CA, January 22-24, 1996.

[11] W.H.W Tuttlebee, "Software-defined radio: facets of a developing technology," *Personal Communications, IEEE*, vol. 6, no. 2, pp. 38-44, April 1999.

[12] S.F. Smith, M. Bobrek, M.R. Moore, and Chen Jin, "Design of an agile radionavigation system using SDR techniques," in *Military Communications Conference, 2005*, 2005, pp. 1127-1132.

[13] J. Zenneck, "Propagation of Plane EM Waves Along a Plane Conducting Surface," *Ann. Phys.*, pp. 846-866, 1907.

[14] A.N. Sommerfeld, "Propagation of Waves in Wireless Telegraphy," *Ann. Phys.*, pp. 665-737, 1909.

[15] K.A. Norton, "The Calculation of Ground-Wave Field Intensity over a Finitely Conducting Spherical Earth," *Proceedings of the IRE*, vol. 29, no. 12, pp. 623-639, December 1941.

[16] G.N. Watson, "The Diffraction of Electric Waves by the Earth," *Proceedings of the Royal Society of London. Series A, Containing Papers of a Mathematical and Physical Character*, vol. 95, no. 666, pp. 83-99, October 1918.

[17] J.R. Wait, "The ancient and modern history of EM ground-wave propagation," *Antennas and Propagation Magazine, IEEE*, vol. 40, no. 5, pp. 7-24, October 1998.

[18] H. Bremmer, "Applications of operational calculus to ground-wave propagation, particularly for long waves," *IRE Transactions on Antennas and Propagation*, vol. 6, no. 3, pp. 267-272, July 1958.

[19] G. Millington and G.A Isted, "Ground-wave propagation over an inhomogeneous smooth earth. Part 2: Experimental evidence and practical implications," *Journal of the Institution of Electrical Engineers*, vol. 1950, no. 7, pp. 190-191, July 1950.

[20] L Sevgi, "A mixed-path groundwave field-strength prediction virtual tool for digital radio broadcast systems in medium and short wave bands," *IEEE Antennas and Propagation Magazine*, vol. 48, no. 4, pp. 19-27, Aug 2006.

[21] R.J Dippy, "Gee: a radio navigational aid," *Journal of the Institution of Electrical Engineers - Part IIIA: Radiolocation*, vol. 93, no. 2, pp. 468-480, 1946.

[22] United States Coast Guard; United States Department of Transportation, *LORAN-C User Handbook*. United States of America, 1992.

[23] J Johler, "The propagation time of a radio pulse," *IEEE Transactions on Antennas and Propagation*, vol. 11, no. 6, pp. 661-668, November 1963.

[24] B.G. Pressey, G.E. Ashwell, and C.S Fowler, "The Measurement of the Phase Velocity of Ground-Wave Propagation at Low Frequencies over a Land Path," *Proceedings of the IEE - Part III: Radio and Communication Engineering*, vol. 100, no. 64, pp. 73-84, March 1953.

[25] Vernon Cooray, "LORAN-C timing errors caused by propagation over finitely conducting ground," *Radio Science*, vol. 24, no. 2, pp. 179-182, March-April 1989.

[26] G.D. Monteath, "Computation of groundwave attenuation over irregular and inhomogeneous ground at low and medium frequencies," The British Broadcasting Corp. Research Department, Engineering Division, 1978.

[27] David Last, Paul Williams, and Kenneth Dykstra, "Propagation of Loran-C signals in irregular terrain - modeling and measurements, Part 1: Modelling," in *International LORAN Association Technical Symposium*, Washington, DC, 2000.

[28] David Last, Paul Williams, and Kenneth Dykstra, "Propagation of Loran-C signals in irregular terrain - Modelling and measurements; Part II: Measurements," in *International LORAN Association Technical Symposium*, Washington, DC, 2000.

[29] David Diggle and Janet Blazyk, "Computer Modeling of LORAN C Additional Secondary Factors," in *Internation LORAN Association 36th Annual Convention and Technical Symposium*, Orlando, FL, 2007.

[30] T Tamir, "On radio-wave propagation in forest environments," *IEEE Transactions on Antennas and Propagation*, vol. 15, no. 6, pp. 806-817, Nov 1967.

[31] H.W. Makarabhiromya, W. Parker, "Electric constants measured in vegetation and in earth at five sites in Thailand," U.S. Army Electronics Command , Fort Monmouth, New Jersey, 1967.

[32] M Le Palud, "Propagation modeling of VHF radio channel in forest environments," in *Military Communications Conference*, 2004, pp. 609-614.

[33] D.L. Sachs and P.J. Wyatt, "A conducting-slab model for electromagnetic propagation within a jungle medium," Defense Research Corporation, Santa Barbara, CA, 1966.

[34] D. Dence and T Tamir, "Radio loss of lateral waves in forest environments," *Radio Science*, vol. 4, no. 4, pp. 307-318, April 1969.

[35] J.R Wait, "Recent analytical investigations of electromagnetic ground wave propagation over inhomogeneous earth models," *Proceedings of the IEEE*, vol. 62, no. 8, pp. 1061- 1072, August 1974.

[36] T.S. Maclean and G Wu, *Radiowave propagation over ground*, 1st ed. London: Chapman & Hall, 1993.

[37] Federal Communications Communication. (2011, June) Federal Communications Commission. [Online]. http://www.fcc.gov/mb/audio/m3/smallm3.jpg

[38] PIC Wire and Cable. (2011, July) Website of PIC Wire and Cable. [Online]. http://www.picwire.com/pdfs/PIC_Technical_Articles/PIC_TA2_Velocity_Factor.pdf

[39] Food and Agriculture Organization of the United Nations. (2011, July) USE OF DEMONSTRATION PROJECTS. [Online]. http://www.fao.org/DOCREP/005/AC660E/ac660e05.htm

[40] S. Swarup and R Tewari, "Depolarization of radio waves in jungle environment," *IEEE Transactions on Antennas and Propagation*, vol. 27, no. 1, pp. 113-116, January 1979.

APPENDICES

APPENDIX A: PATH PROFILES

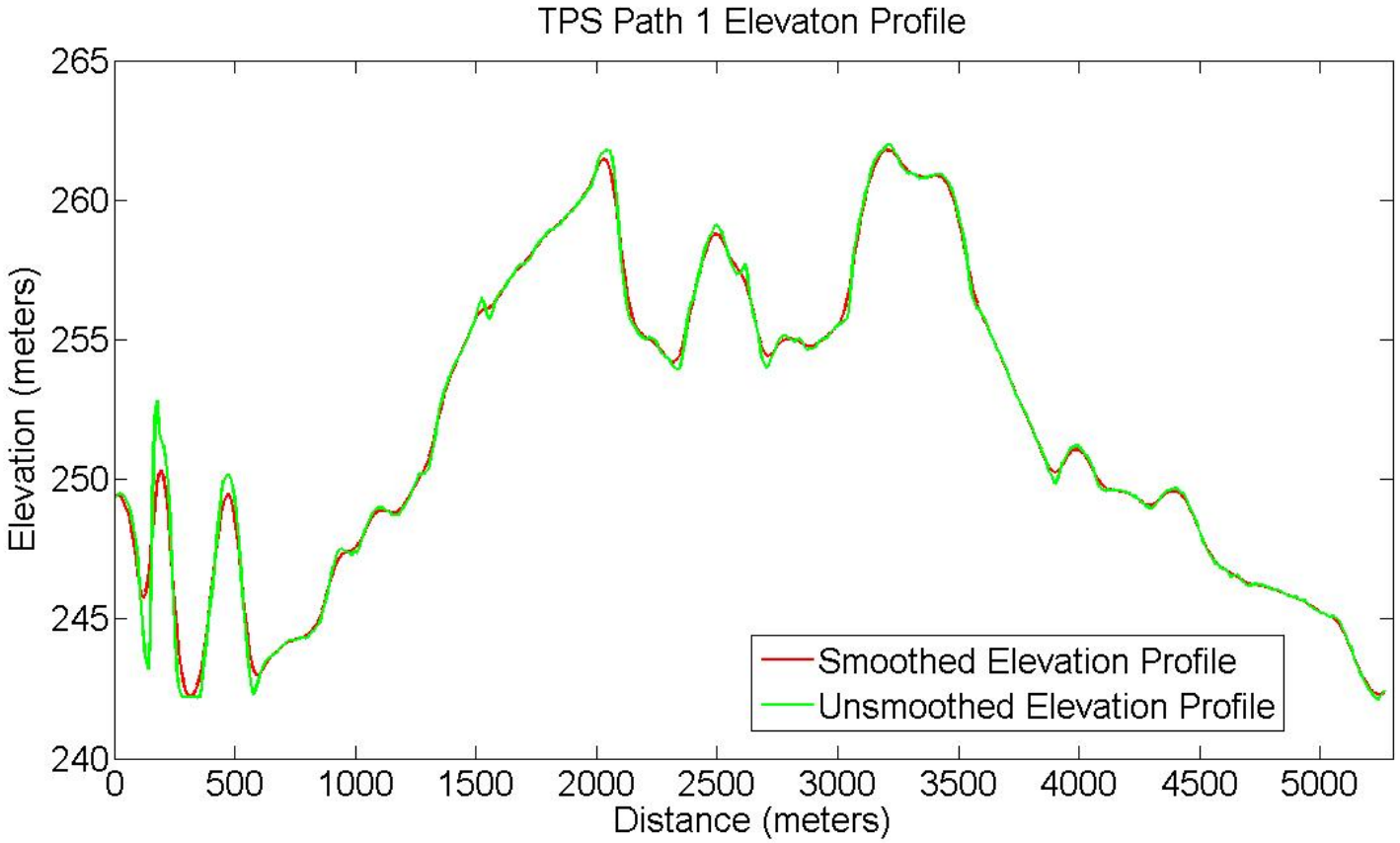

Figure 24 - Elevation profile for TPS path 1 depicting both the unsmoothed and the smoothed terrain profiles. The smoothed profile was used for calculation of surface impedance perturbation.

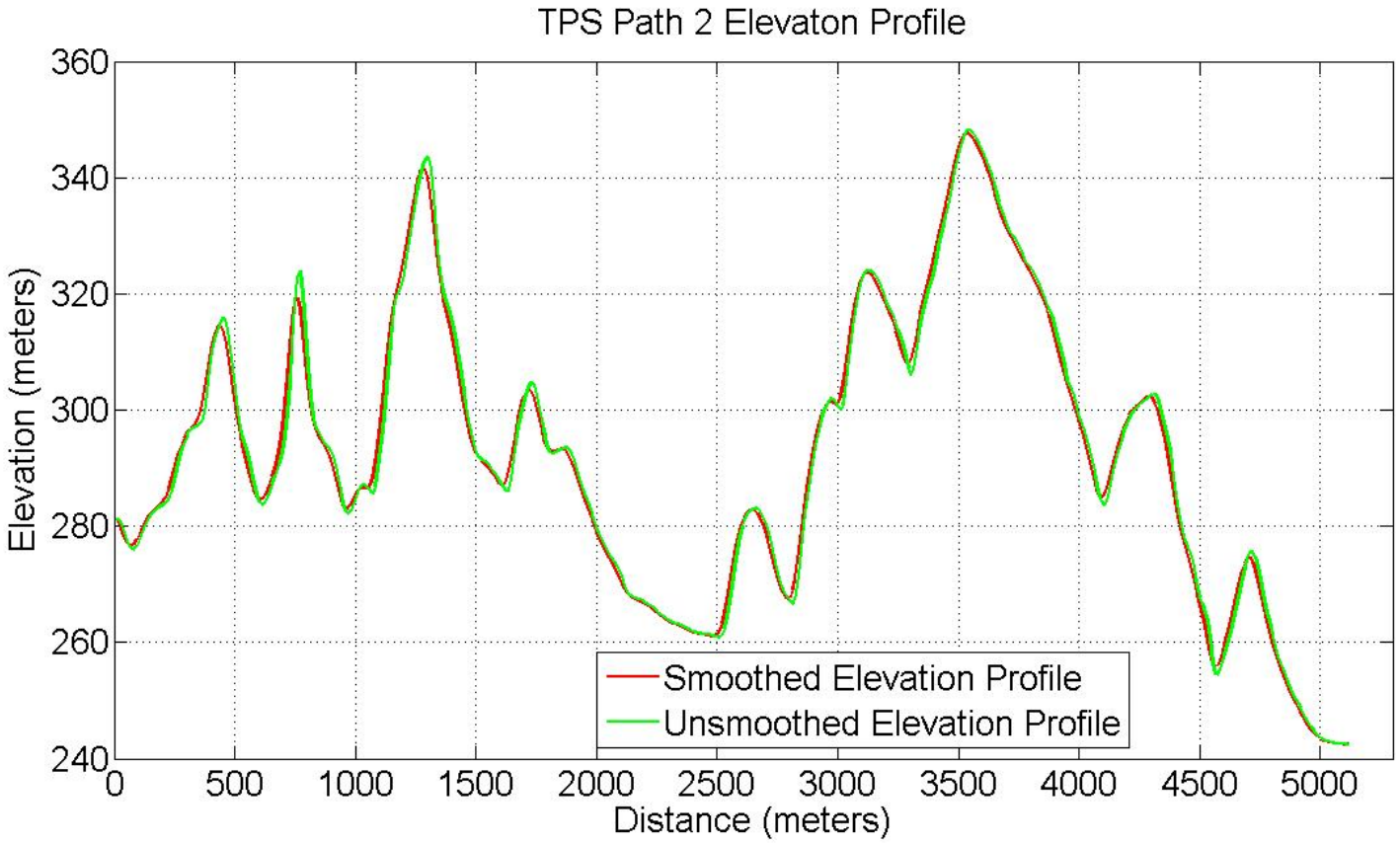

Figure 25 - Elevation profile for TPS path 2 depicting both the unsmoothed and the smoothed terrain profiles. The smoothed profile was used for calculation of surface impedance perturbation.

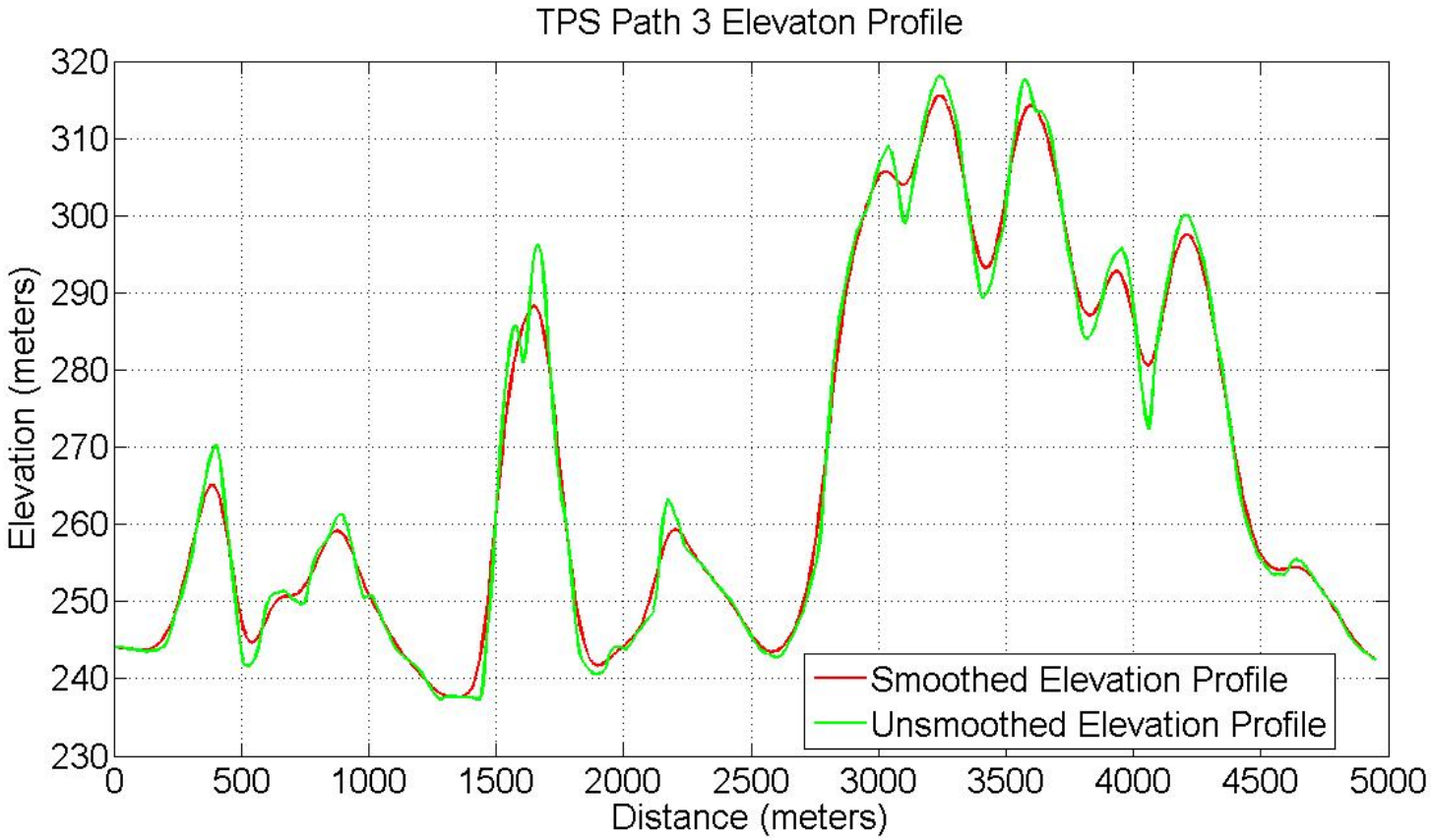

Figure 26 - Elevation profile for TPS path 3 depicting both the unsmoothed and the smoothed terrain profiles. The smoothed profile was used for calculation of surface impedance perturbation.

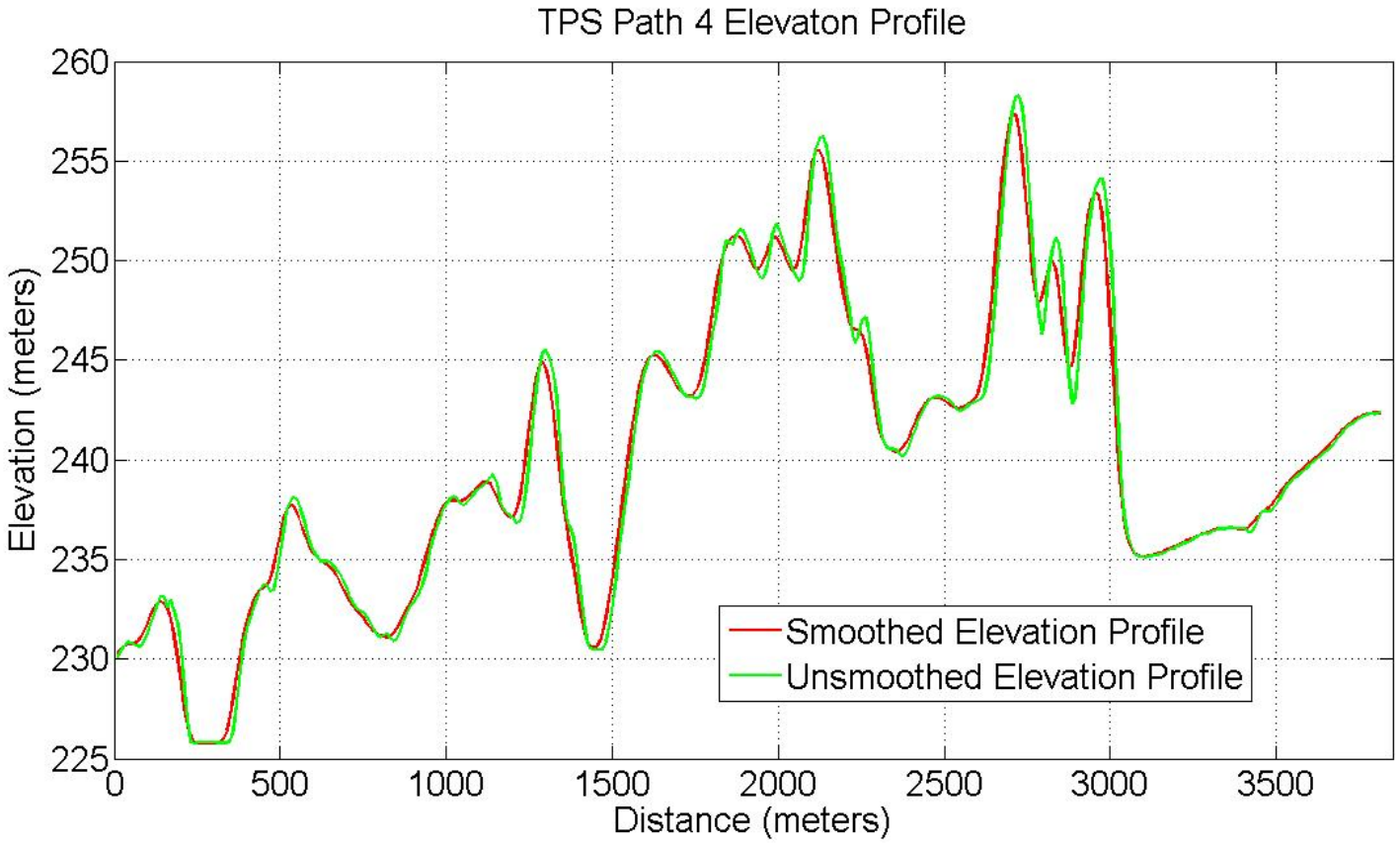

Figure 27 - Elevation profile for TPS path 4 depicting both the unsmoothed and the smoothed terrain profiles. The smoothed profile was used for calculation of surface impedance perturbation.

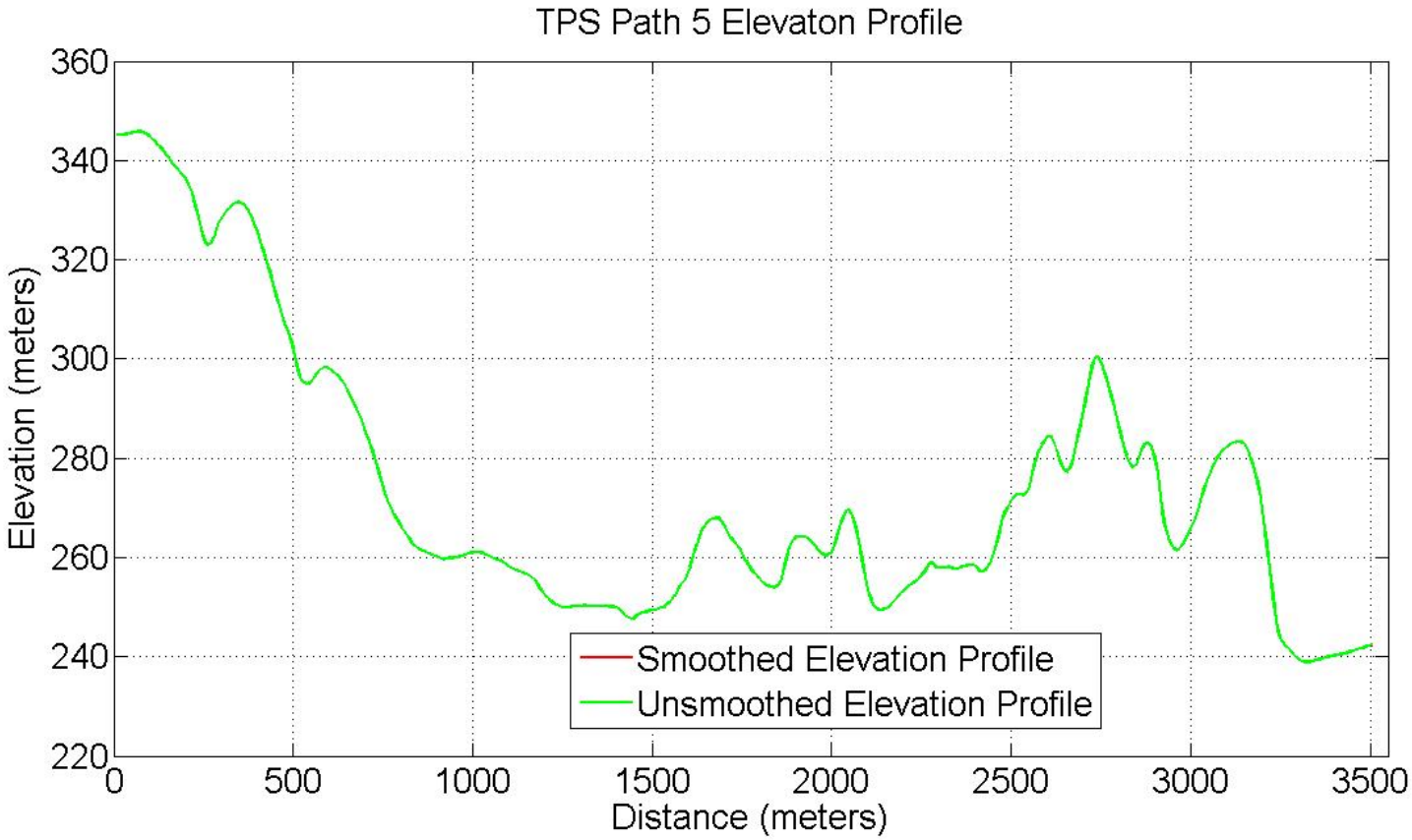

Figure 28 - Elevation profile for TPS path 5 depicting both the unsmoothed and the smoothed terrain profiles. The smoothed profile was used for calculation of surface impedance perturbation.

VITA

Zachary Michael Crane was born August 3, 1987 in Knoxville, TN. He grew up in the Knoxville area where he was Homeschooled through grades K-12. He was accepted to the University of Tennessee to study Engineering, starting in the Fall of 2005. During his freshman studies, he was convinced by the focus of his interests and faculty presentations to choose Electrical Engineering and formally entered the University of Tennessee EECS department in the Spring of 2006. Beginning in the Fall of 2007, Zack spent a total of 3 semesters as a Co-Op engineering student with ExxonMobil Corp in Beaumont, TX. His activities there included instrument reliability projects, new instrument installations, and hurricane recovery work. Having completed his tenure at ExxonMobil, he returned to Knoxville to put his experience to work for students by serving for the 2009-2010 academic year as a Co-Op ambassador for the University of Tennessee Office of Professional Practice. He graduated with his B.S. in Electrical Engineering in May of 2010. He began his graduate studies in Electrical Engineering with a focus on Electromagnetic Propagation in May 2010, and also worked as a Graduate Teaching Assistant for 3 semesters, designing and organizing Software Defined Radio projects for seniors studying Digital Communication Theory. Zack married his wife, Shannon Danae Gardner on August 5th, 2011, and has accepted a position as an Electromagnetic Compatibility Engineer with Analysis and Measurement Services in Knoxville. He will begin working at AMS in January of 2012.